Evaluation of transiert tracer measurements from three cruises to the Mauritanian upwelling region: estimation of transit time distribution and ventilation

Dissertation

Mian LIU

Primary advisor: Prof. Dr. Martin Visbeck

Second advisor: Dr. Toste Tanhua

GEOMAR
Helmholtz-Zentrum für Ozeanforschung Kiel

Department of Chemical Oceanography

Helmholtz-Zentrum für Ozeanforschung Kiel

Kiel University, Kiel, Germany

November 2012

CATALOG

Summary

Mauritanian upwelling region is located in subtropical Atlantic, off the northwest African shore. The parameters of seawater (e.g. temperature, salinity and oxygen) have certain impacts on the biological processes and the fisheries production. Tracer gases (CFC-12 and SF6) are used to show the mean age and distribution of water masses and then to measure the ventilation from upwelling and currents near the Mauritanian coast. In this thesis, I report the measurements of tracer gases from three cruises (different years and seasons) along the latitude of 18 °N. The analysis shows the following results:

Seasonal variation of sea surface temperature (SST) and sea surface salinity (SSS) is directly influenced by solar radiation and wind stress. Salinity, whose distribution is similar with temperature, is highest in summer but lowest in spring instead of winter due to the precipitation.

Oxygen concentration in seawater is a result of both physical and biological processes:

1) Solubility, which decreases with temperature, is highest in winter and lowest in summer.

2) Upwelling, which is strong in winter and early spring, can bring water from oxygen minimum zone (OMZ) to the surface.

3) Ventilation process depends on currents, which is strong in winter.

4) Apparent oxygen utilization (AOU) under the euphotic layer is low in spring.

As a final result of all the above reasons, the oxygen concentration is highest in winter and lowest in summer.

Transit time distribution (TTD) of tracer gases is used to show the distribution and movement of water masses. A value of $(\Delta/\Gamma) = 1.4$ is chosen to show the mixing rate in the ocean. Since concentration and partial pressure of tracer gases have disadvantages to show the age of water masses, saturation of tracer gases in the seawater are used to calculate the mean age. According to the mean age and direction of water movement at the upper layer, this area can be divided into two parts by the longitude of 17 °W:

1) The upwelling has impacts on the near coastal region, where the mean age is relative old at the upper layer (east of 17 °W). During the upwelling season (spring and winter), water with old mean age is transported from deeper layer to the surface. The upwelling is strong in winter and early spring because the monsoon blows from land to sea and transports the surface water off the coast. As a result, temperature and salinity at surface is relative lower compared with the open ocean. Oxygen concentration is also influenced by the upwelling. Water from OMZ (200 to 500m depth) is transported upwards, so water samples with low oxygen in the upper layer can be found near the coast.

2) The currents (such as NECC and NEUC) influence the open ocean area, where the mean age is relative young at the upper layer (west of 17 °W). Stratification is relative clear and the vertical water exchange in this region is not so obvious as the coastal region. Water from SEC and NBC is transported eastward by trade wind and forms the NECC and NEUC, which ventilate the subtropical North Atlantic. The currents are strongest in winter due to the trade wind. Temperature and salinity decrease with depth. Oxygen concentration is relative lower in the east because the NECC and NEUC with oxygen-rich water come from the west.

1. Introduction

1.1 Motivation

Upwelling is one of the most interesting phenomena in oceanography, because it can transport water, which has high nutrient, low temperature and low pH value, to the surface. In the upwelling region, high nutrients (e.g. nitrogen) can be brought to the upper layer (Schafstall et al., 2010; Kock et al., 2011) and fisheries can be formed (e.g. Fisheries in Mauritanian and Peru). Low temperature along the west coast has certain impact on the El Nino. And the pH value of seawater is one component of carbon cycle (Cao et al., 2007).

Since the mixing and the differences of temperature and the salinity between water masses, it is difficult to measure each process that happens in the ocean, so the tracer elements, such as CFC-12 and SF_6, can be used to label the upwelling and water masses that we are interested in (Fine, 2010).

Another result of the upwelling is that it can transport water with low oxygen concentration, which can definitely influence the biological density in the ocean, to the upper layer. The concentration of oxygen in the ocean, which is determined by the solubility, apparent oxygen utilization (AOU) (Karstenson et al., 2008) and the ventilation process (Brandt et al., 2010), is also an important parameter of the water self-purification capacity.

Mauritanian upwelling region, which is also one of the most famous fisheries, is located to the northwest coast of Africa. In this thesis, the upwelling process and its impact on the ventilation will be discussed.

1.2 Wind-driven Upwelling near the Mauritanian Coast

There are different kinds of upwelling, such as: coastal upwelling and equatorial upwelling. Coastal upwelling is known to be the most common type, and most is induced by wind.

According to the Ekman Theory, the wind stress induces a surface flow of 45°to the right in the North Hemisphere (left in the South Hemisphere), and the whole transport is 90°to the right (North Hemisphere) (Ekman, 1905). And most of the Ekman transport happens within the upper tens of meters, relative shallower in summer and deeper in winter (Price et al., 1987).

The Mathematical Equations are as follows:

$$\frac{1}{\rho}\frac{\partial}{\partial z}\tau_x = -fv,$$

$$\frac{1}{\rho}\frac{\partial}{\partial z}\tau_y = fu,$$

(where τ is the wind stress near the surface, ρ is the density of seawater, u and v are the zonal and meridional velocity.)

The Mauritanian Coast (about 18 °N) is located on the north boundary of the Inter-Tropical Convergence Zone (ITCZ) in summer (Philander et al., 1995), the wind stress blows from the Northeast, so the water in the upper layer is transported to the Northwest and away from the coast, and finally induces an upwelling. The seasonal difference is also obvious. More wind-driven coastal upwelling is induced because of the stronger wind stress in winter and early spring (Mittelstaedt, 1991). The upwelling near the Mauritanian coast is dominated by wind stress.

1.3 Ventilation Process in the upwelling region

Seawater from Oxygen Minimum Zone (OMZ) is transported by upwelling to the surface. Before we measure the oxygen concentration in the upwelling region, the situation from the OMZ should be explained and some background knowledge about the subtropical Atlantic is also required:

1.3.1 Oxygen Minimum Zone (OMZ):

OMZ has the lowest oxygen concentration and it appears usually between 200 to 1000m depth in the ocean (Paulmier et al., 2009). The oxygen in the surface water is close to equilibrium to the atmosphere, and the organic tissues are produced by the photosynthesis. During the fall of these organic tissues, oxygen will be consumed by the aerobic bacteria and most tissues will be used within 1000m depth. The seawater deeper than 1000m has higher oxygen solubility, because of the lower temperature. And the exchange with the bottom water from Antarctic, which is rich in oxygen, can also help to raise the oxygen content (Stramma et al., 2005).

Mauritanian upwelling region is in the eastern of the subtropical Atlantic. Besides the above-mentioned reasons (Stramma et al., 2008), the ventilation by Subtropical Cells (STCs) should also be considered:

Most of the tropical and subtropical Atlantic seawater (especially in the western basin) is ventilated by the NEC (North Equator Current) and the SEC (South Equator Current), but both of them do not go through the eastern basin (west coast of Africa). The connection between them is the Subtropical Cells STCs (Schott et al., 2004).

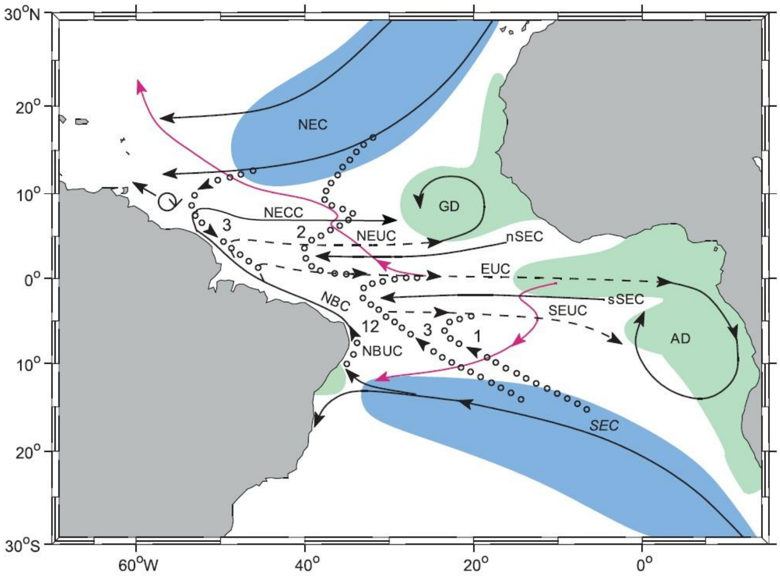

Figure 1.0 (a) Subtropical Cells (STCs) in Atlantic. (Schott et al., 2004)

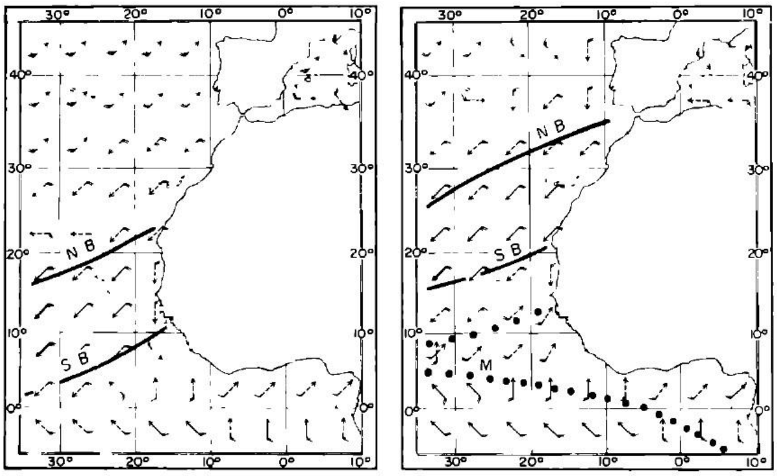

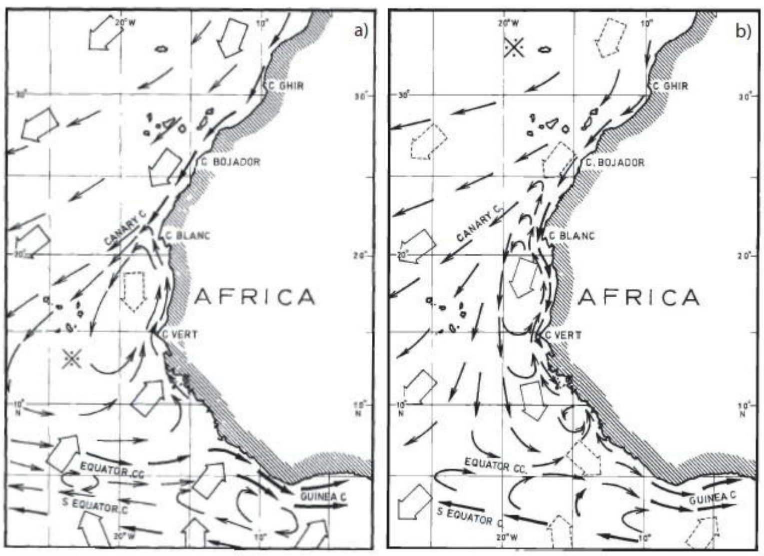

Fig 1.0 (b) and (c) Seasonal Variation of Wind Stress (b) and Upwelling Undercurrent (c) (Mittelstaedt, 1991)

1.3.2 Currents

As mentioned in the Introduction Section (Fig 1.0), the currents have important impacts on the ventilation in the Subtropical Atlantic (Hazeleger, 2003). In this region, the water is ventilated by the STCs and the strength of NECC and NEUC, which belongs to the STCs, can definitely influence the oxygen concentration (Schott et al., 2004).

North Equatorial Counter-Current (NECC):
The NECC flows between the North Equator Current (NEC) and South Equator Current (SEC) and is induced by trade wind in the Inter-tropical Convergence Zone (ITCZ). NECC flows from west to east at the surface, and transports water with high oxygen, which comes from North Brazil Current (NBC) (Bourles et al., 1999), to the eastern basin of subtropical Atlantic. The seasonal difference of NECC is significant (Stramma et al., 1999). It begins in summer (May and June), reaches its maximum in autumn and early winter then gets weaker and finally disappears in late winter or early spring.

North Equatorial under-Current (NEUC):
The NEUC, which origins most from the south Atlantic (SEC) and partly from the north Atlantic (NEC), flows also eastwards at the same depth as thermocline (Hazeleger et al., 2003). And its depth has a seasonal variability as well as the mixed layer depth. NEUC is another current, which ventilates the eastern basin of subtropical Atlantic, and it carries deeper and colder water than NECC (about 5 ℃ colder).

In local scale, the North Equator Current (NEC) goes westward at the 18 °N, the region of Mauritanian eastern coast is ventilated by the North Equator Counter Current (NECC) and North Equator Under Current (NEUC), which belong to the current branches of STCs and come from the American eastern coast. As both NECC and NEUC have weaker transport and take a longer time, the ventilation process in the eastern basin is weaker and slower.

Upwelling undercurrent (UUC):
In this region, the upwelling undercurrent (UUC) is one of the features in subtropical North Atlantic Ocean (Mittelstaedt, 1983; Barton et al., 1998). It flows northward between Cape Vent and Cape Blanc, along the Mauritanian continental slope at surface and subsurface (see Fig 1.0 (c)) (Mittelstaedt, 1991).
The seasonal variation of UUC is also obvious due to the change of trade winds (Mittelstaedt 1983). In winter, trade winds blow strongly from the Northeast, and induce a drift current, which flows southward and along the shoreline. So the UUC is shifted to the west, some distance away from the shore (Mittelstaedt and Hamann, 1981). Also, the UUC is shifted by the southward current into the subsurface layer and cannot be detective at surface. During its way to the north, UUC upwells because of Ekman transport.
In summer, the southward current disappears, the UUC returns to the surface and gets closer to the shore. Less upwelling can be found because the trade winds from the northeast are weaker.

Atlantic Meridional Overturning Circulation (AMOC):
AMOC is a large-scale thermohaline (Kuhlbrodt et al., 2007) circulation in Atlantic. Seawater with high density is formed in north Atlantic, where the temperature is low and salinity is high, and leads to a buoyancy loss. North Atlantic Deep Water (NADW) is formed during the down-welling and then transports to the south in the deep. At the surface, warm water flows northward. The whole AMOC leads to a net northward heat flux in the Atlantic Ocean (Ganachand and Wunsch, 2000).

In subtropical Atlantic, the STCs (including NECC and NEUC) and the AMOC interact with each other and influence the temperature, salinity, oxygen concentration by physical processes.

Guinea Dome:
Since NEC and SEC, which carry cold and oxygen-rich water from mid-latitude towards the equator, do not go through and ventilate the eastern basin of subtropical Atlantic, the oxygen concentration in this region is relative low and two oxygen minimum zones are formed: Guinea Dome in the north and Angola Dome in the south (Siedler, 1992; Stramma et al., 2005). The Mauritania coast (18 °N) locates in the Guinea Dome.

1.3.3 Water Masses

Three water masses are found in the upper layer of this region (Stramma et al., 2005).

Mixed Layer Water
The mixed layer locates at the upper layer of the ocean. Seawater from mixed layer has the highest temperature, salinity and oxygen concentration. The Mixed Layer Depth (MLD) and its seasonal variation can be measured with CTD profiles (Thomson et al., 2003 and Montegut et al., 2004). In this region, the MLD is within 100m depth.

Central Water
The central water is made up with north Atlantic central water (NACW) and south Atlantic central water (SACW) (Stramma et al., 1998). They can be found with a linear T-S relationship, and contact each other at Cape Verde Frontal Zone, which locates between latitude 16 and 20 °N. Water from NACW has higher temperature and salinity than SACW. The depth of central water is between 150m to 600m. The oxygen concentration is the lowest, and NACW is also higher than SACW.

Antarctic Intermediate Water (AAIW):
AAIW is formed at the latitude between 50 and 60 °S, and then transported to the tropical region by the subtropical gyre (Stramma et al., 1998). Then, near the northeastern coast of south American, AAIW is carried by north Brazil current (NBC) and NEUC and finally approaches the eastern basin of north Atlantic. During the transport, AAIW can be

recognized by its low temperature and salinity. In the eastern basin of subtropical Atlantic, AAIW is found between the depth between 500m and 1000m. The concentration of oxygen in this water mass is relative higher than central water.

1.4 Transient Tracer elements

All the above currents and water masses flow in the ocean basin at the same time. The whole situation is complex and, as mentioned before, it is difficult to measure each process. Tracer elements are used here to label the water masses we are interested in. There are different tracer elements with different methods to measure:

1) Conserved Transient Tracers:

The concentration of this kind of tracer elements in the atmosphere increases (or decreases) monotonously in the history, and their surface concentration depends on time (Fine, 2010). So from measuring the concentration in the water masses, we can calculate that, to which year from the atmospheric history it is equilibrium, and how many years did it take to move from surface into the deep ocean. (The method will be mentioned in the next section).

Examples: CFC-12 and SF_6

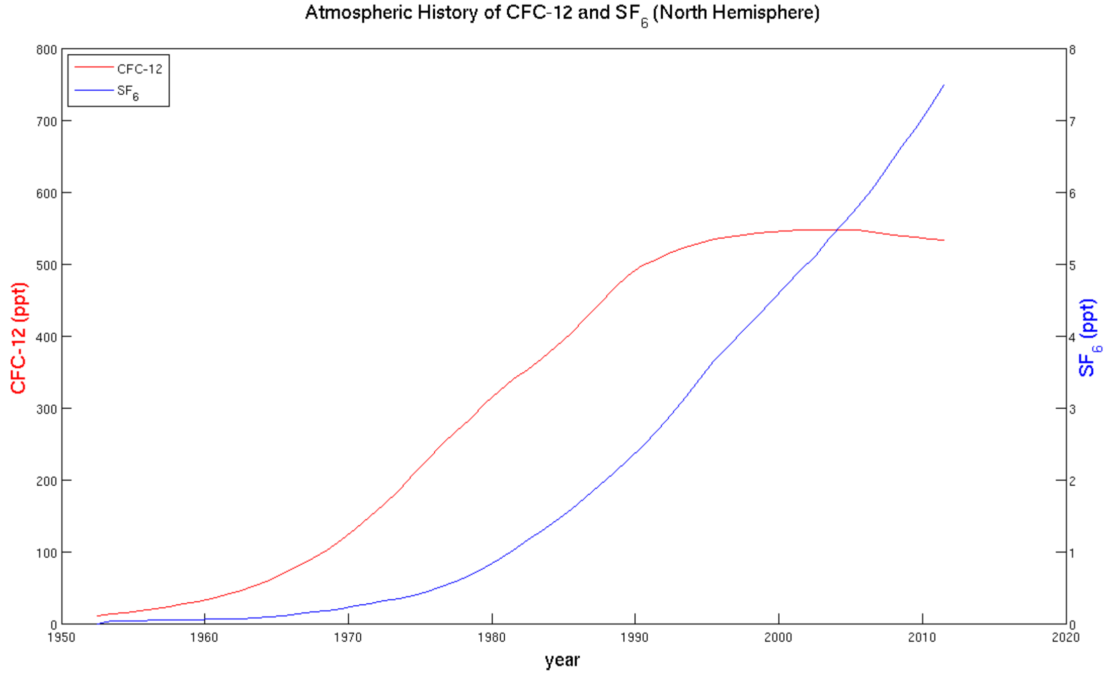

Figure 1.1 Atmospheric histories of conserved tracers in North Hemisphere

There is also a little difference between the North and the South Hemisphere (see figure below), due to the human action. In this region (18°N), historical data from North Hemisphere is used.

2) Radioactive Tracers:
The concentration at the surface can be measured. But the value goes down with time at a certain rate because of the decay. With the original surface concentration and the decay rate, the age of the water mass and their history are able to be calculated. (for example: Tritium (Müller, 1977) and Helium (Craig and Lupton, 1982))

In this thesis, the conserved transient tracers (CFC-12 and SF_6) are used.

1.5 Transit Time Distribution (TTD)

Since the mixing in the ocean, it is difficult to measure the whole process in one timescale. The transit time distribution is a better choice to measure. There are several parameters of the TTD:

1) The time, which the water takes from surface to the deeper layer. And for each water particle, it has its own time that can be defined as "tracer age" (τ).
2) For the conserved tracers, it is possible to calculate the year, in which the water mass is equilibrium to the atmosphere, since the concentration in the atmospheric history increases monotonously and can be found in the reference. This "year" can be defined as "mean age" (Γ).
3) The "width" (Δ) and the "mixing ratio" (Δ/Γ) shows the mixing and the diffusion in the ocean.

In the mathematics, the "tracer age", the "mean age" and the "width" can be calculated as follows Waugh et al., (2003):

Tracer age: $c(t) = c_0(t\text{-}\tau)$,

(where c_0 is the surface concentration, c is the deeper concentration, τ is the tracer age.)

Mean age: $\Gamma = \int_0^\infty \xi G(\xi) d\xi$

(where Γ is the mean age, ξ is the time, and G is the Green function)

Width: $\Delta^2 = \frac{1}{2}\int_0^\infty (\xi - \Gamma)^2 G(\xi) d\xi$,

The relationship between all the above parameters is often assumed to follow an inverse Gauss distribution (Waugh et al., 2003):

$$G(t) = \sqrt{\frac{\Gamma^3}{4\pi\Delta^2 t^3}} \exp\left(\frac{-\Gamma(t-\Gamma)^2}{4\Delta^2 t}\right)$$

(Where t is the tracer age and the mean age is 90 years.)

We can see in the Figure 1.2, G(t) appears as the inverse Gauss distribution, and with the increasing Δ/Γ, the "peak" appears earlier and the "tail" is longer.

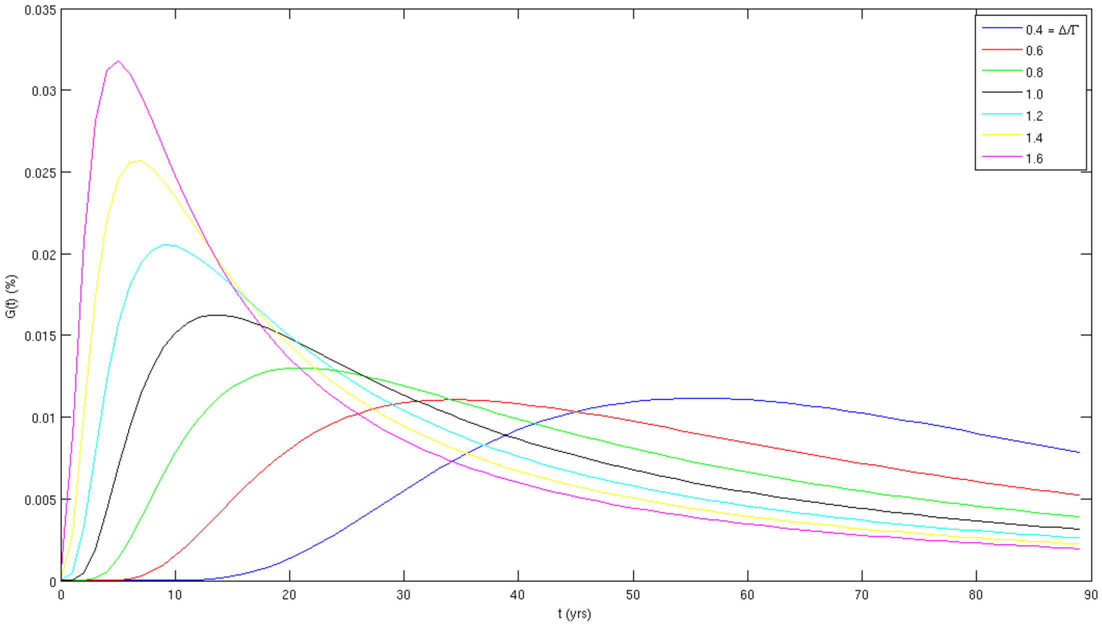

Figure 1.2 inverse Gauss distribution with different Δ/Γ

The suitable choice of "mixing ratio" (Δ/Γ) can help to increase the accuracy. (More information in the data and method section)

1.6 How to choose the tracer:

Each tracer (CFC-12 and SF_6) has its own advantages and uncertainties in measurement (Tanhua et al., 2008). In the calculation, there is a little difference between the mean age based on different tracers. And this difference increases with the value of (Δ/Γ).
(See Figure 1.3 below):

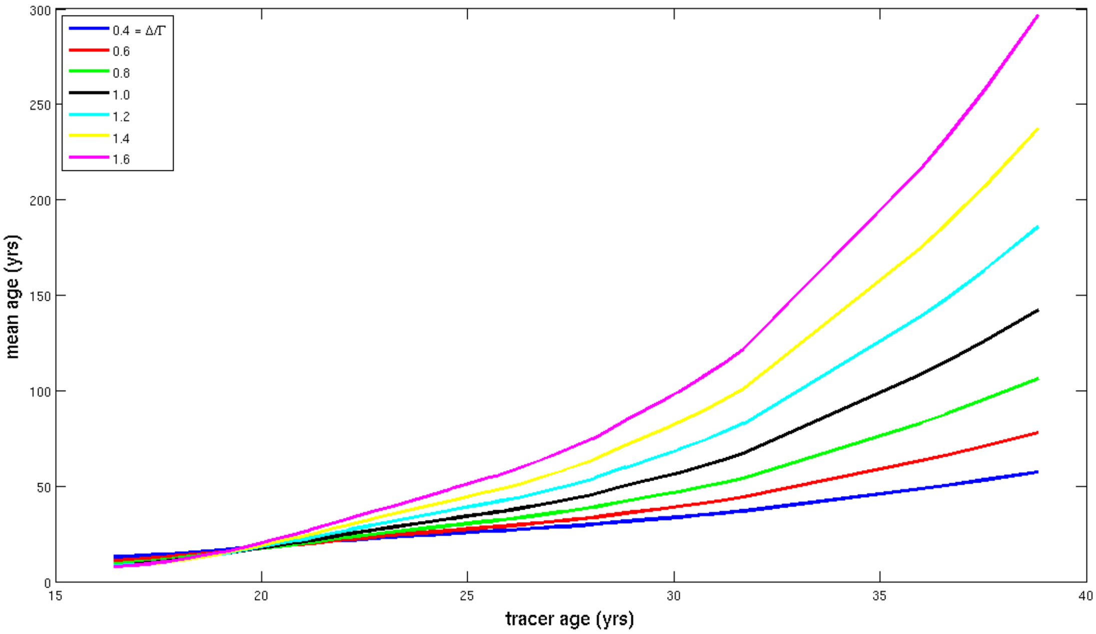

Figure 1.3(a) relationship between tracer age and mean age based on CFC-12

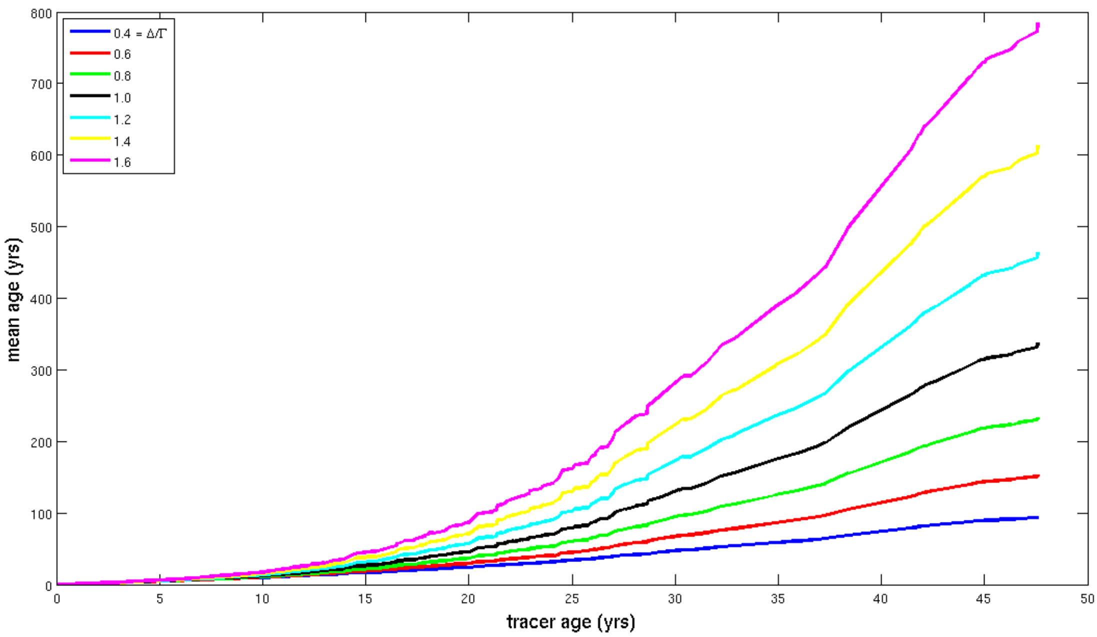

Figure 1.3(b) relationship between tracer age and mean age based on SF_6

As we can see in the figure above (Figure 1.1), the concentration of CFC-12 in atmospheric history increased until early 1990s, and decreased from 2000s. As a result, for the recently formed water masses (pCFC-12>450ppt), the uncertainties based on CFC-12 increases, the SF_6 is the better choice. On the other hand, the relative error will increase in the deeper layer, as the absolute concentration of SF_6 is pretty low in both atmosphere and seawater.

2. Data and Method

2.1 Cruises and stations

Data from three cruises in different years (2005, 2006, 2007) and different seasons (spring, summer, winter) are analyzed.

2.1.1 Poseidon 320

The cruise Poseidon 320 traveled from March 21st to April 7th (spring) in subtropical Atlantic. Between the latitudes of 17.5 °N and 18.5 °N, three groups of data were taken, including 4 stations at the latitude of 17.5 °N, without tracer data; 6 stations at the latitude of 18 °N (one station at 19 °W with tracer data) and 6 stations at 18.5 °N with tracer data (Bange et al., 2005).

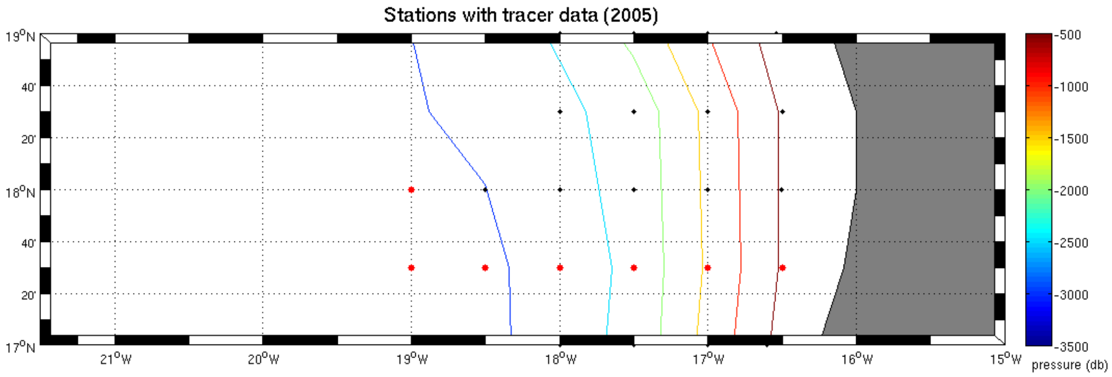

Fig 2.1 Stations of Poseidon 320 (spring, 2005) are shown in this figure. Data from this cruise covers the area between 17.5 °N and 18.5 °N, 16.5 °W and 19 °W. Red dots are stations with tracer data (CFC-12 and SF_6), whereas black dots show the stations without tracer data.

2.1.2 Meteor 68

The cruise Meteor 68 traveled from April 26th to August 7th (summer), 2006 in Atlantic. The interaction between ocean surface and low atmosphere in the region of Mauritanian upwelling are measured. Samples from 11 stations at the latitude of 18 °N were taken, including four stations of tracer elements (CFC-12 and SF6) (Koschinsky et al., 2006).

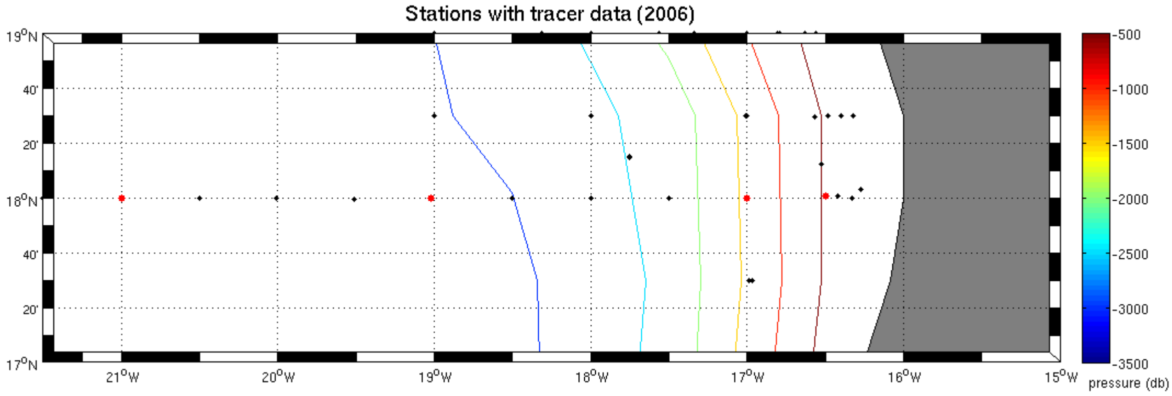

Fig 2.2 Stations of Meteor 68 (summer, 2006) are shown in this figure. Data from this cruise covers the area between 17.5 °N and 18.5 °N, 16.3 °W and 21 °W. Red dots are stations with tracer data (CFC-12 and SF_6), whereas black dots show the stations without tracer data.

2.1.3 Poseidon 347

The cruise of Poseidon 347 lasted from January 18th to February 5th (winter), 2007 and covered a box between 18.5 °N, 17.5 °W (northwest) and 17.5 °N,16.25 °W (south east), the Mauritanian upwelling region is included in the box. 572 data from 59 stations were sampled, including 8 stations with CFC-12 and SF_6 data (Dengler et al., 2008).

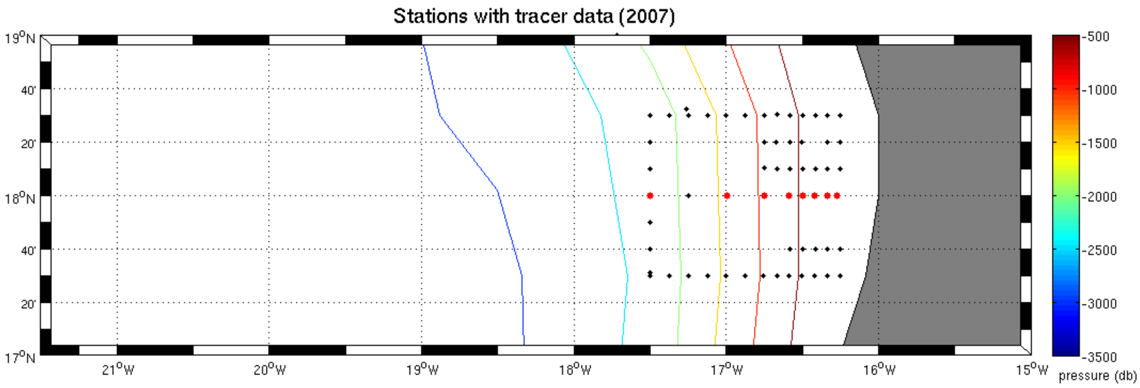

Fig 2.3 Stations of Poseidon 347 (winter, 2007) are shown in this figure. Data from this cruise covers the area between 17.5 °N and 18.5 °N, 16.2 °W and 17.5 °W. Red dots are stations with tracer data (CFC-12 and SF_6), whereas black dots show the stations without tracer data.

2.2 Measurements:

CTD-O2 measurements

The Seabird systems (SEB-2, SEB-3 and SEB-5) were used to measure the conductivity, temperature and pressure (CTD). The pressure was measured with one sensor (s/n 80024), but the temperature, conductivity and oxygen concentration were measured respectively with two independent sensors ((s/n 2826) and (s/n 4547) for temperature, (s/n 2512) and (s/n 2859) for conductivity, (s/n 0194) and (s/n 0992) for oxygen).
From Cape Verde to the Mauritanian coast, samples were taken between surface and 1300m depth (5 stations to the bottom because the seafloor is shallower than 1300m). Along the Mauritanian coast, samples were taken from surface to 1000m deep or to the bottom when the total depth is shallow (less than 1000m).
The pressure and the temperature calibration were done in the laboratory before and after the cruise.
The salinity is based on the result of conductivity (using the Guildline Autosal Instrument) and all the analysis of salinity was done at night because of the constant air temperature.
The concentration of oxygen was done by the Winkler titration method.

Tracer gases

Measurement of tracer gases has two steps:

First step is to purge the dissolved gas from water samples. There are two different systems in this step:
In the lab: The flame sealed water samples were taken back to the lab for later analysis. Ampoules are heated firstly, so that the dissolved gas is released into the headspace. Then the cracker is flushed with clean nitrogen until the air is removed.
In this thesis, the system in the lab is used. There is another system but not used:
(On board: The chamber is evacuated until the inside pressure is lower than 5 mbar. Then the water sample is sucked into the chamber, leaving a space in the top, and the gas is purged from water sample with clean nitrogen.)

After flushing, the next step can be started.

The second step is to trap the gas:
The purge flow goes through the chamber and the tracer elements (CFC-12 and SF_6), which dissolved in the water sample, will be trapped in the purge flow. During this step, also two different systems are used:
Packed column system: Gas from purge system goes firstly pass a nafion dryer and magnesium perchlorate to get dried and then enter the trap. The trap is filled with Haysep D and cooled with liquid nitrogen to the temperature of -70 ℃. When the purge flow passes the trap, the gas is absorbed. Then the trap is heated and the gas is released in to the precolumn filled with Prosasil C. After backflushing the precolumn, the gas is separated in

the main column packed with Carbograph (180 cm) and molecular sieve 5 Å (20 cm).
Capillary column system: The first part is similar with packed column system. After the precolumn, the gas is trapped in the second trap, which is smaller than the first, before it goes into the main column. The main column is much longer and thinner, which is formed by DB 624 (75 m) and RT-molecular sieve 5 Å (30 m).
In this thesis, most of the samples are measured with packed column system, and the samples measured with capillary column system will be reanalyzed.
The main column is connected to the Electron Capture Detector (ECD).

2.3 Choice of data

The data were "flagged" after measurements.
Flag = 2, means the data is good,
Flag = 3, means the data is probably bad,
Flag = 4, means the data is known to be bad,
Flag = 7, means the data is measured by capillary system and will be "reflagged" later.

Firstly, the water samples need to be "reflagged" before they were analyzed after they were taken back to the laboratory.

For example: the data from station 68, 2005:
The blue points are the original data, which are measured with capillary column system and would be recognized again and then "reflagged" to be "good" (red) or "bad" (green) data.

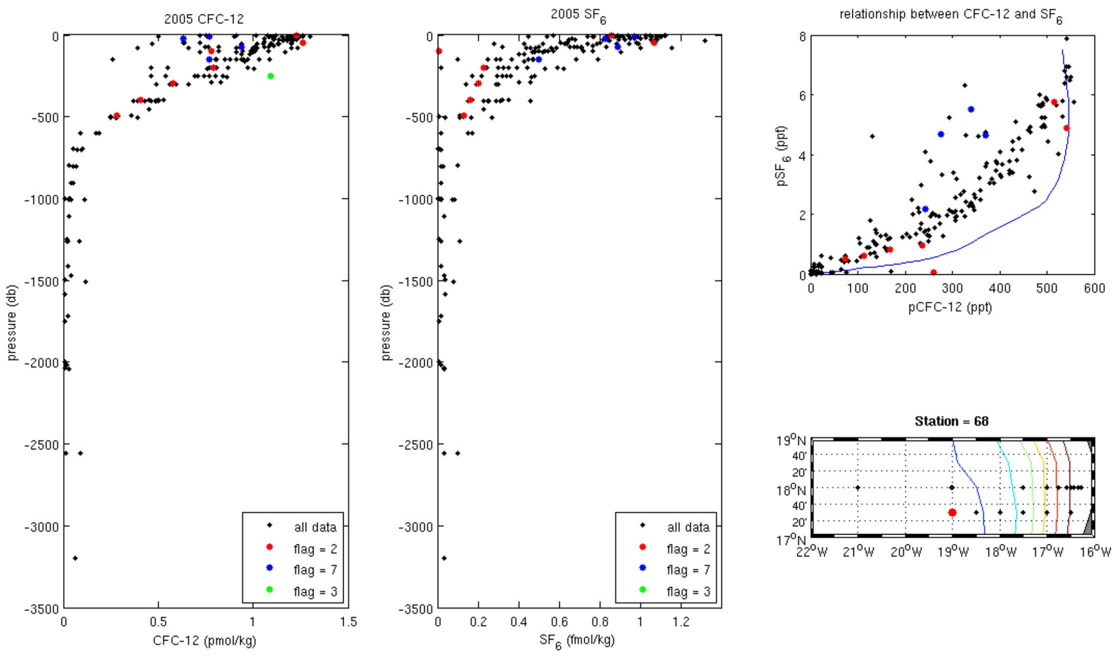

a) The original data:

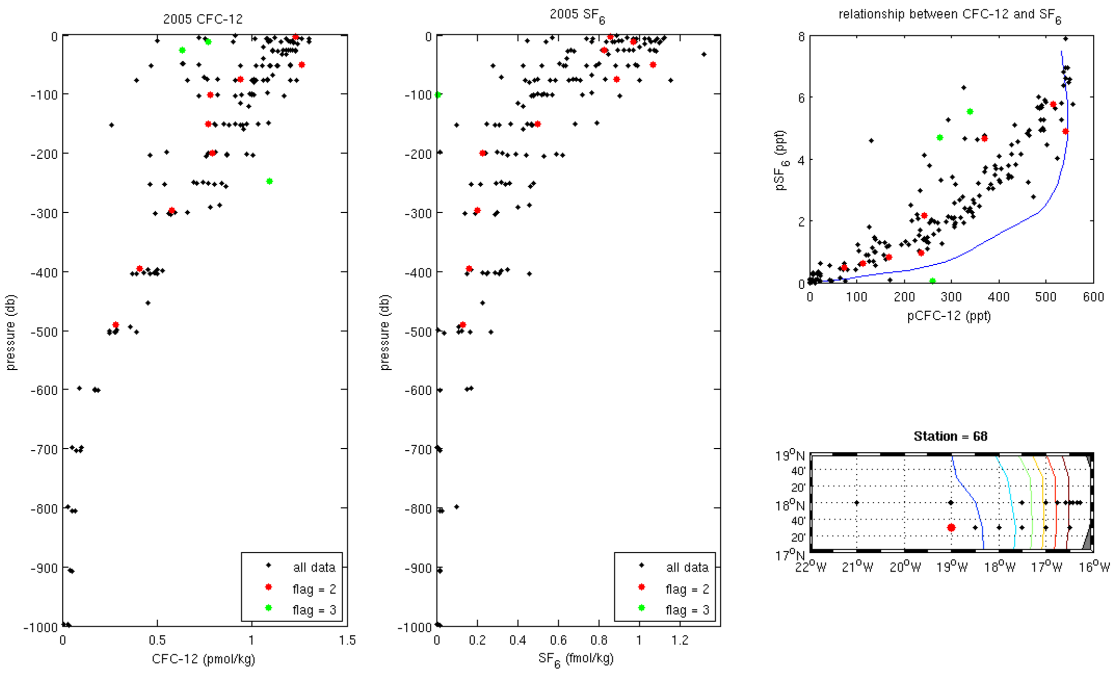

b) "reflagged" data

Fig 2.4 The black points are all the data from current cruise (Poseidon 320, 2005). The points of other colour show the data from current station (station 68, 2005), where red means "good" (flag=2), green means "probably bad" (flag=3), blue means "measured with capillary system" (flag=7). The blue line in the third figure (top-right) shows us the ratio between CFC-12 and SF_6 in the atmospheric history. The points should follow this line if there is NO mixing in the ocean. The map on the bottom right shows the current station with red point.

And the "reflagged" of data is based on Tanhua et al., 2008, the distribution of partial pressure of CFC-12 and SF_6 should follow the blue line if there is NO mixing in the ocean. But in fact, the mixing ratio is usually not zero, so the dots are some distance away from the line and a suitable mixing ratio should be chosen.
After "reflagging", there is no blue points on the profile and all the "good" data (red points) would be analyzed in the next section.

2.4 Choice of mixing ratio

As mentioned in the introduction section, the value of (Δ/Γ) shows us the one-dimensional mixing and the diffusion in the ocean. In the idealized situation, the mean age based on CFC-12 and SF_6 should have the same value if there is no mixing. But in fact, there will be difference between them because of the different mixing rate in different time and regions. So a suitable value of (Δ/Γ) should be chosen for each time and region, so that the difference could be the minimum.

The following figures show us the mean age of two tracers with different ratios.
All the three years have very similar values, it means that the mixing in this region does not change very much during these three years.
From 0.4 to 1.2, the mean age based on CFC-12 is obvious larger than that based on SF_6, and if we choose 1.6, the mean age will be too large and the standard deviation will increase. For the deep water (under 300m depth), the concentration of SF_6 is very low, so the accuracy is also low. We consider mostly the upper water to decide the mixing ratio (Δ/Γ).
As a result, the value of 1.4 for (Δ/Γ) is considered to be a suitable value for the mixing ratio during the three years.

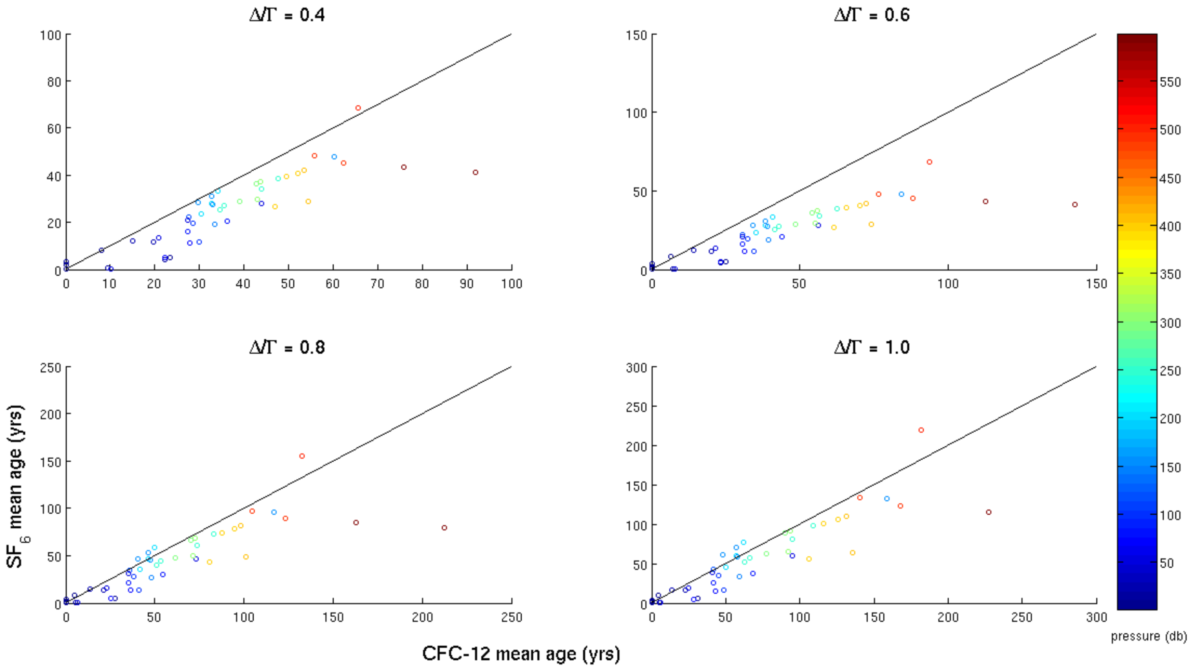

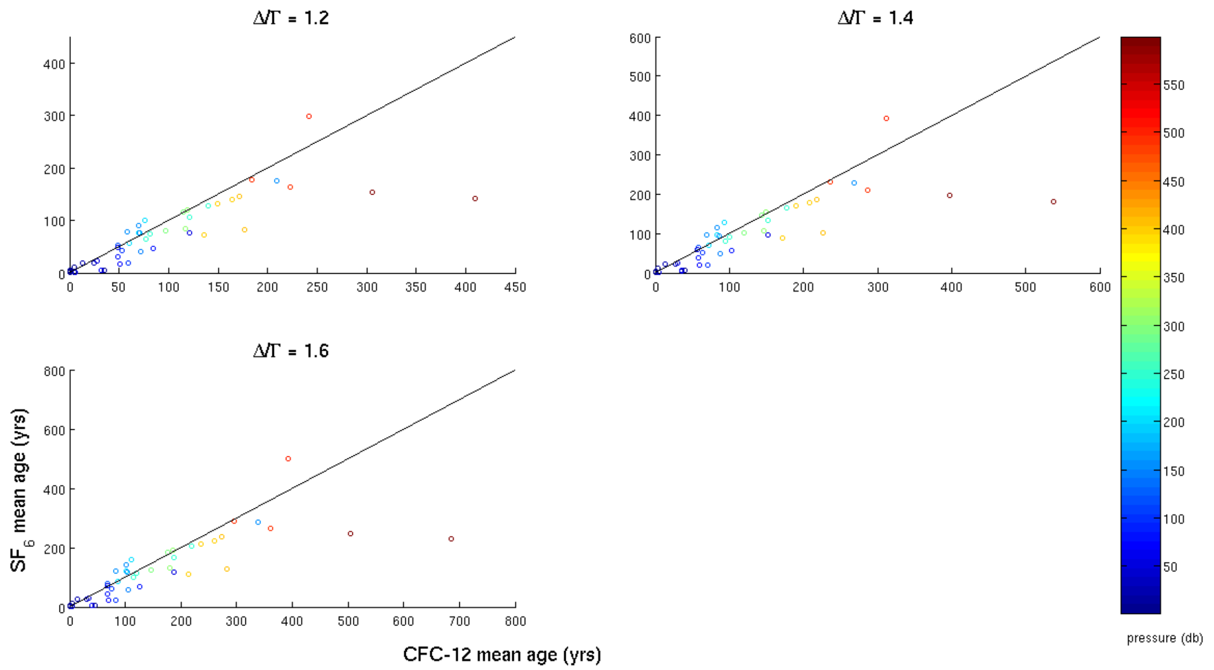
Δ/Γ = 1.2
Δ/Γ = 1.4
Δ/Γ = 1.6
SF6 mean age (yrs)
CFC-12 mean age (yrs)
pressure (db)

a) 2005

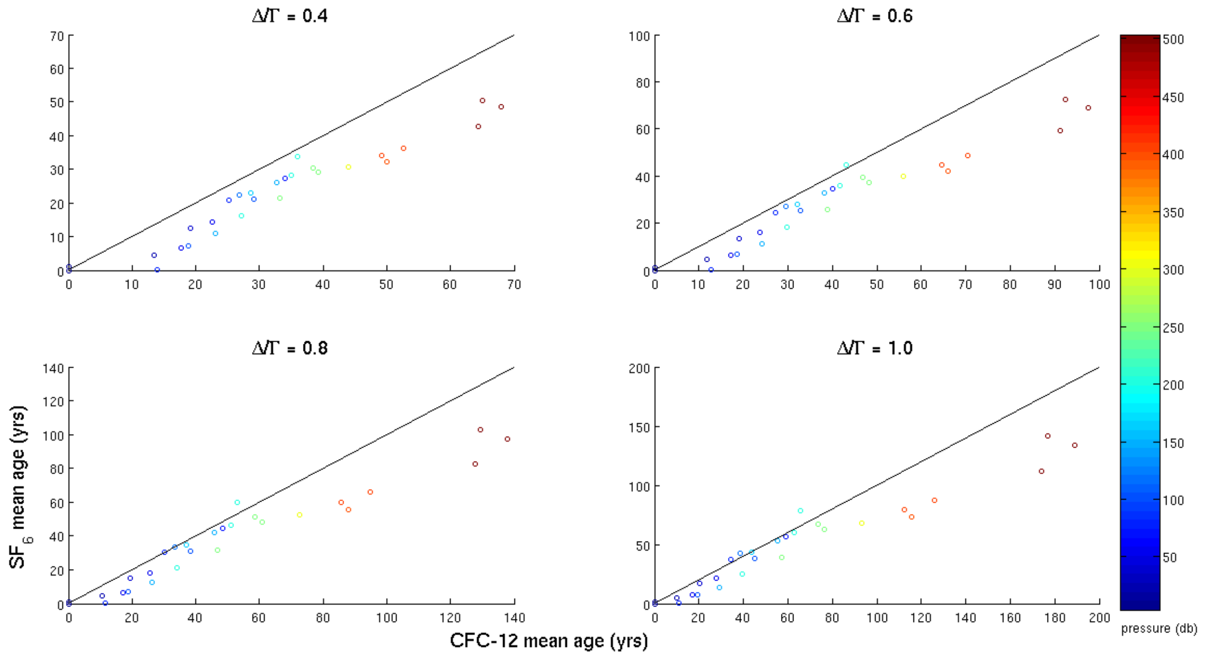
Δ/Γ = 0.4
Δ/Γ = 0.6
Δ/Γ = 0.8
Δ/Γ = 1.0
SF6 mean age (yrs)
CFC-12 mean age (yrs)
pressure (db)

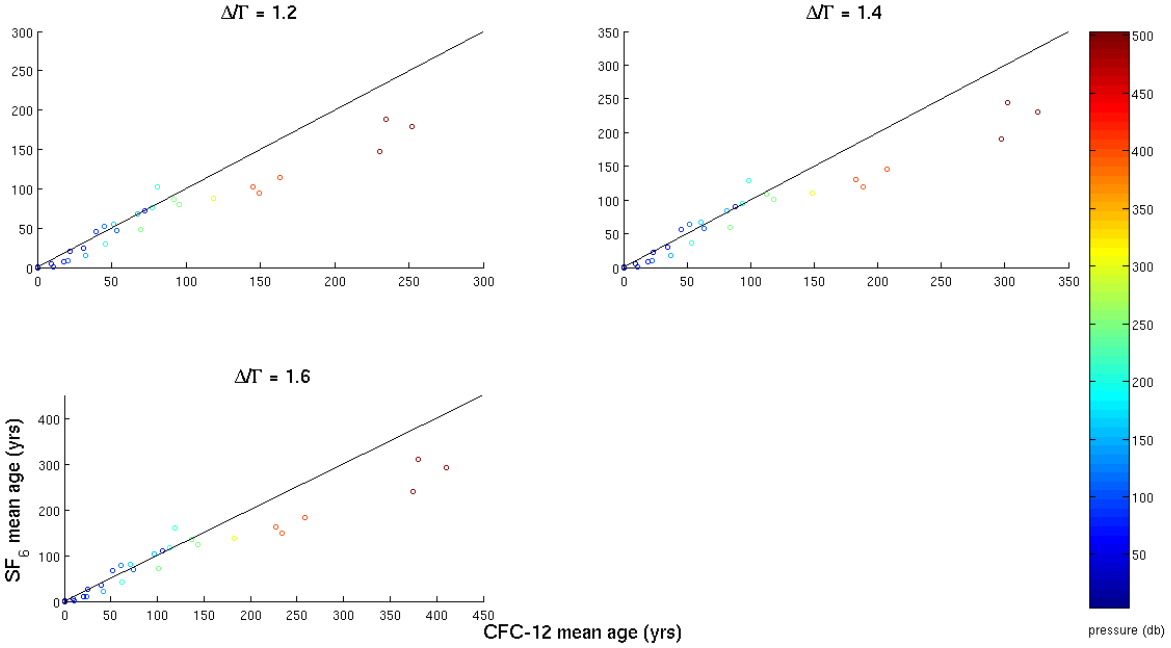
Δ/Γ = 1.2
Δ/Γ = 1.4
Δ/Γ = 1.6
SF$_6$ mean age (yrs)
CFC-12 mean age (yrs)
pressure (db)

b) 2006

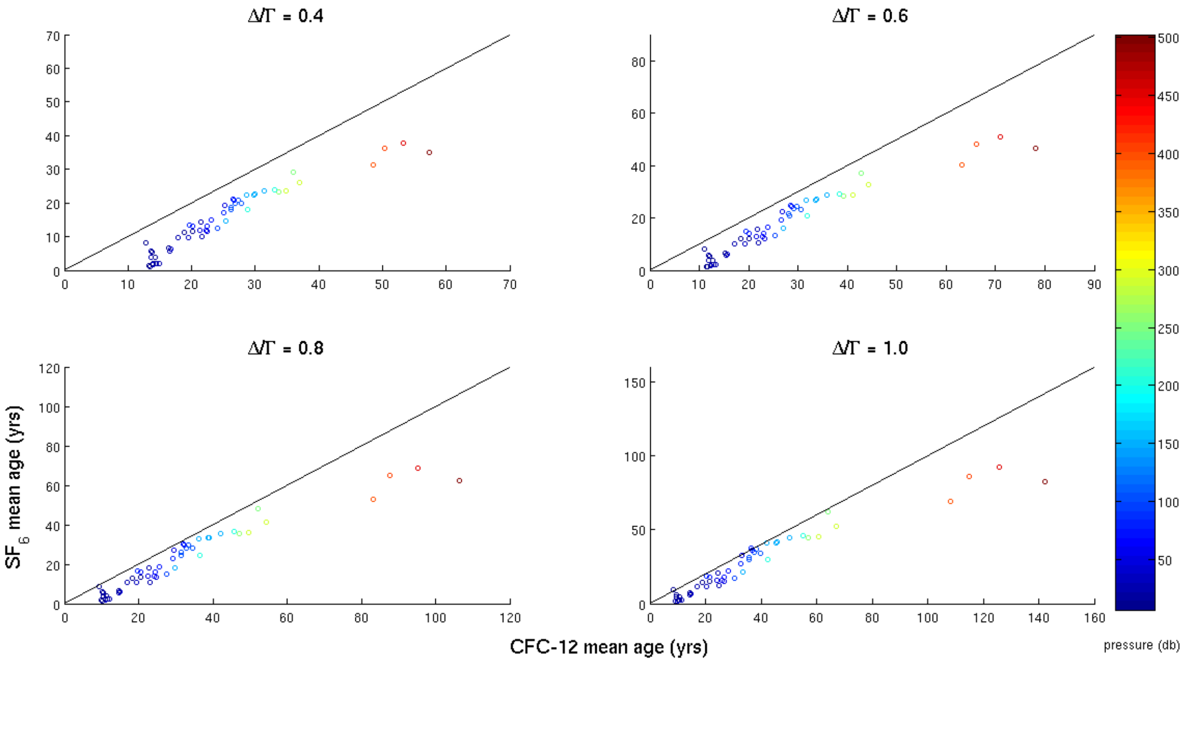
Δ/Γ = 0.4
Δ/Γ = 0.6
Δ/Γ = 0.8
Δ/Γ = 1.0
SF$_6$ mean age (yrs)
CFC-12 mean age (yrs)
pressure (db)

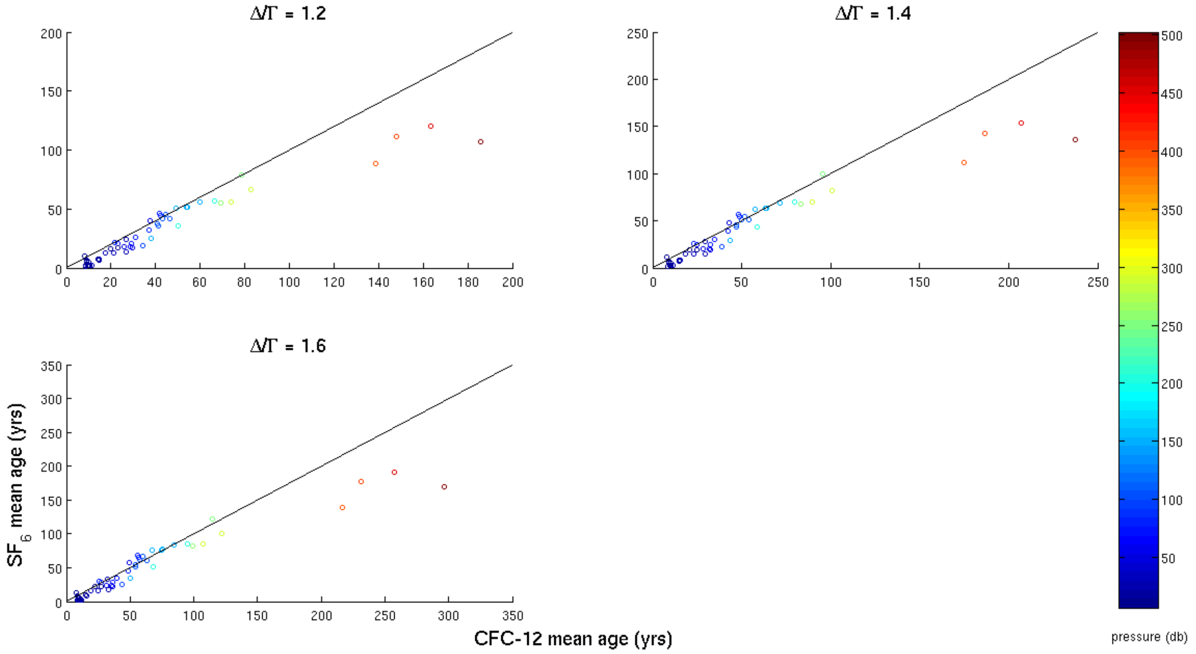

c) 2007

Fig 2.5 This figure shows the relationship between mean age based on CFC-12 and SF_6 with different mixing ratio in three different seasons and years.

3. Results

3.1 Mean state

Fig 3.1 show us the mean states of all the 3 years and large differences can be seen between the coastal region (east of 17 °W) and the open ocean area (west of 17 °W):

2005: The temperature and salinity decreases with depth. Both of them are higher in the open ocean (20 °C and 35.9) than near the coast (17 °C and 35.7). At the depth of 1000m, the minimum of salinity shows the AAIW. The oxygen concentration at surface is also higher in the open ocean (220 μmol/kg) than coastal region (180-200 μmol/kg). The OMZ appears between 200 and 500m. In the deep ocean, the oxygen concentration increases and the maximum appears at the depth of about 2000m.
2006: In summer of 2006, the temperature reaches its maximum and the difference between the open ocean and coastal region is small (both of them are 23 °C). The salinity is higher in the open ocean (36.2) than the coastal region (36). The minimum of salinity also appears at the depth of 1000m. The oxygen concentration at surface is low in summer (200 μmol/kg). The OMZ locates also between the depth of 200 and 500m. The maximum of oxygen in the deep ocean is at the depth of 2500m.
2007: In winter of 2007, the temperature is lowest (19 °C in the open ocean and 17 °C near the coast). The salinity in these two regions are 36.1 and 35.8. The oxygen concentration is over 220 at surface and the OMZ locates deeper than other two seasons (300 to 500m depth). Water samples with low oxygen are also found in the shallow zone (100 to 200m depth) near the coast.
Let us divide the figures into two parts by depth and see their differences:

In the upper layer:

1) Temperature and Salinity:

The distribution of temperature and salinity are similar. Both of them reduce with depth. The sea surface temperature (SST) is about 23 °C in summer and 19 °C in winter. The maximum of salinity exists at surface, and the value of sea surface salinity (SSS) is about 36 (higher in summer (36.3) and lower in winter (36.1)). NECC flows at surface and transports water with high temperature and salinity eastwards until 17 °W. As a result, it plays an important role of the SST and SSS in the region west than 17 °W.
The thermocline (halocline) exists at about 100-300m depth, and the temperature and salinity have a reduction of about 5 °C and 0.4. NEUC flows eastwards at this depth and carries relative warm and salty water (cooler and fresher than NECC) also until 17 °W.
Near the coastal region (east than 17 °W), upwelling has a certain impact of the SST

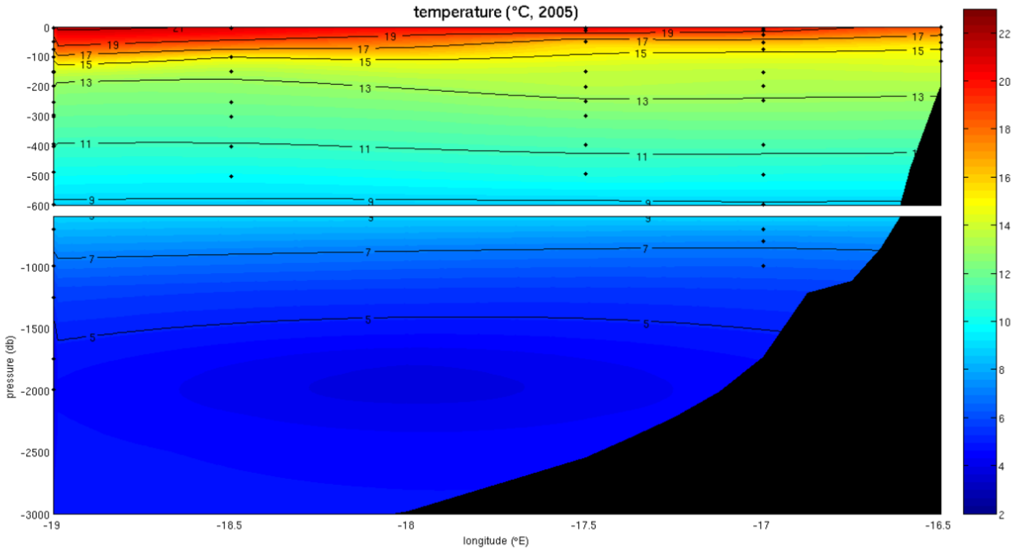
temperature (°C, 2005)
pressure (db)
longitude (°E)
-19
-18.5
-18
-17.5
-17
-16.5

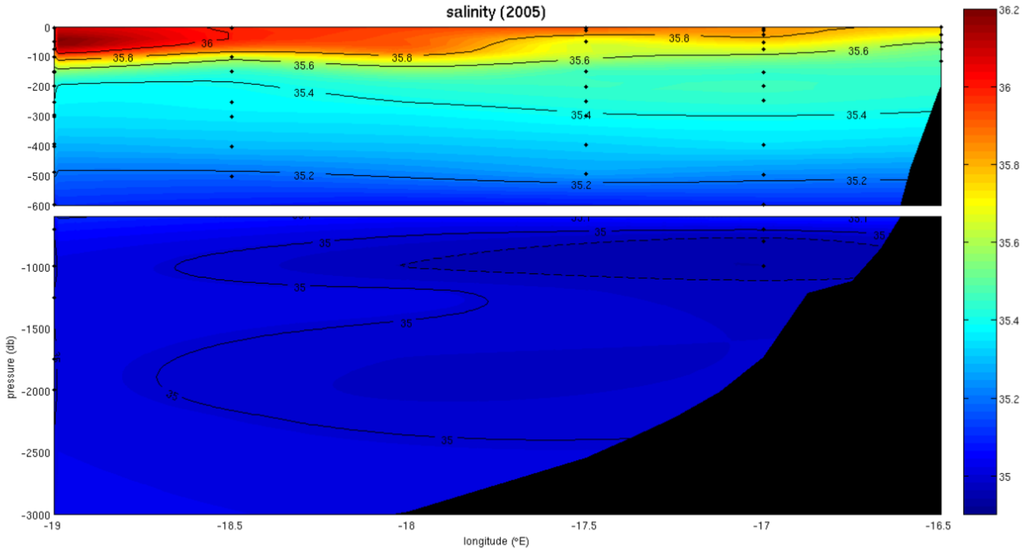
salinity (2005)
pressure (db)
longitude (°E)
-19
-18.5
-18
-17.5
-17
-16.5

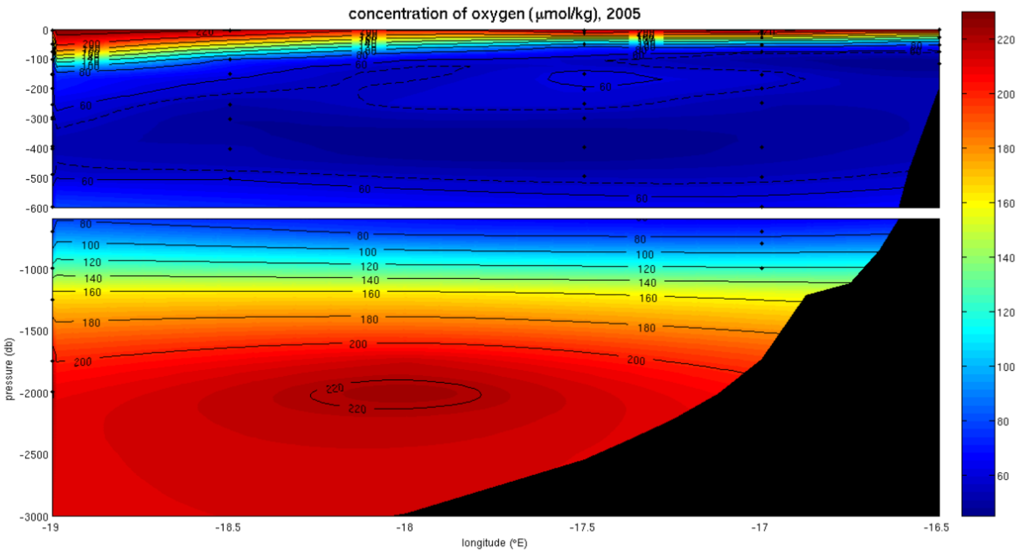
concentration of oxygen (μmol/kg), 2005
pressure (db)
longitude (°E)
-19
-18.5
-18
-17.5
-17
-16.5

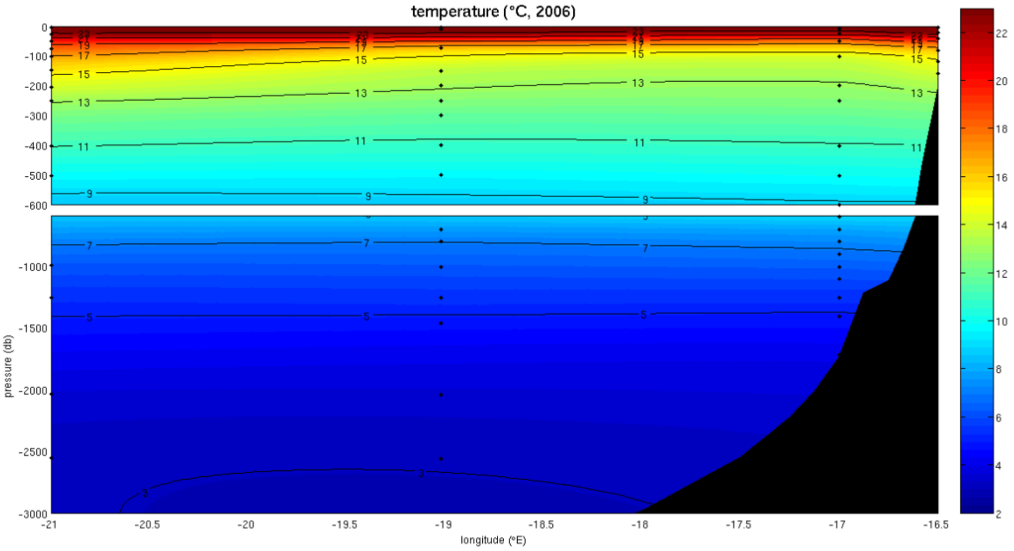
temperature (°C, 2006)
pressure (db)
longitude (°E)

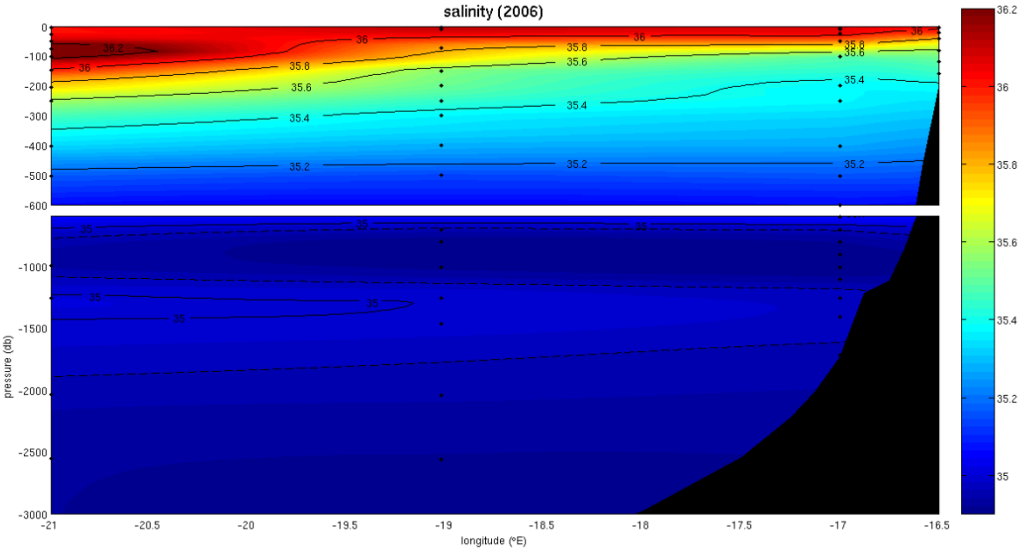
salinity (2006)
pressure (db)
longitude (°E)

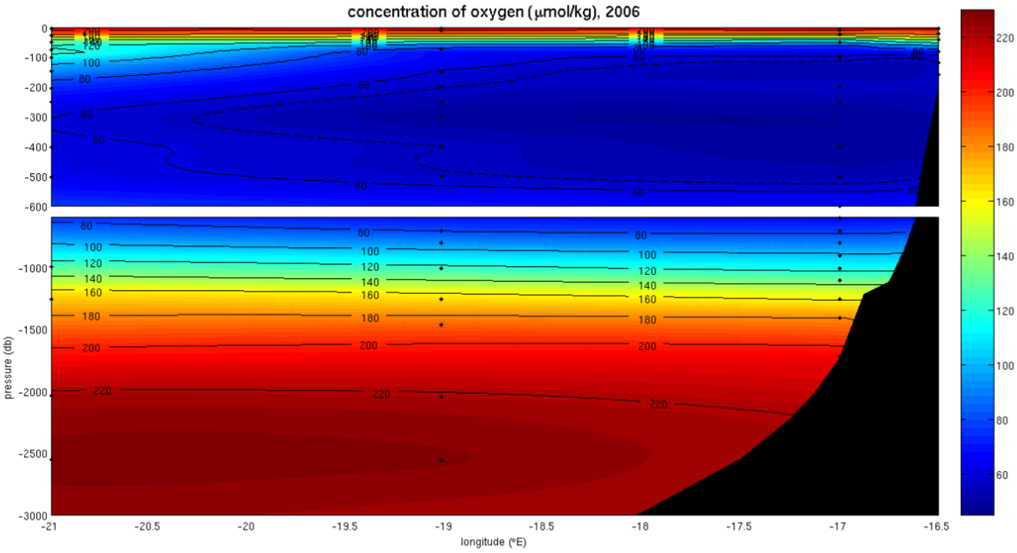
concentration of oxygen (μmol/kg), 2006
pressure (db)
longitude (°E)

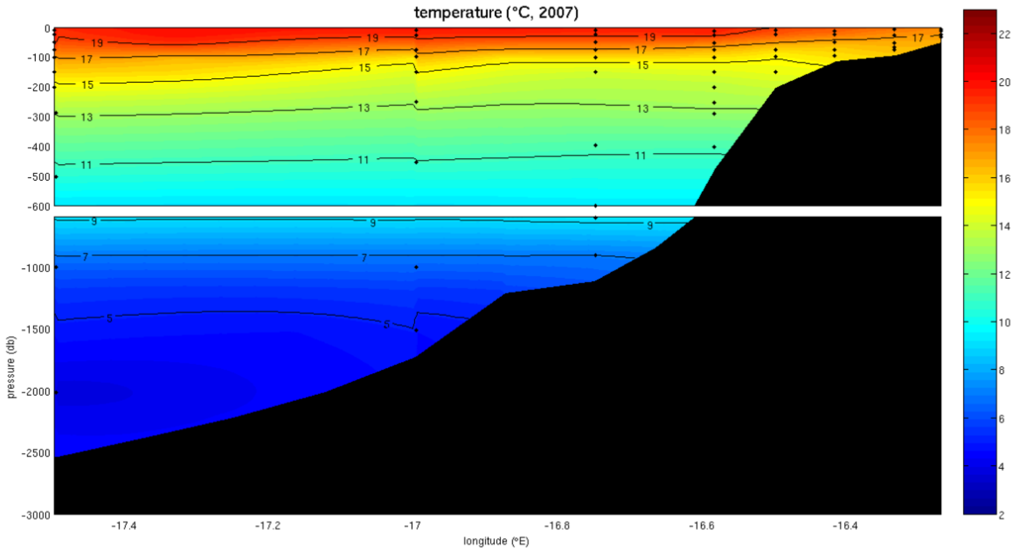
temperature (°C, 2007)
pressure (db)
longitude (°E)

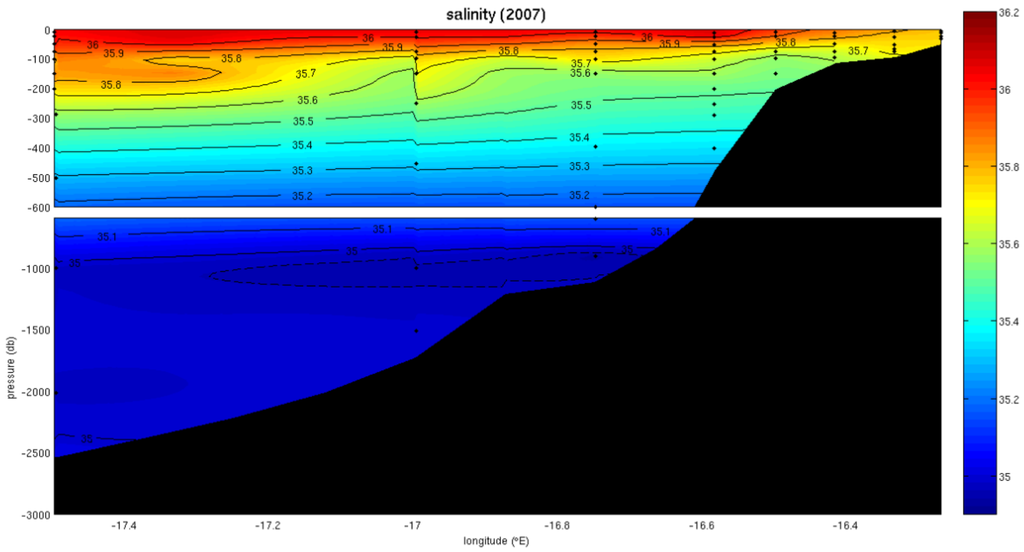
salinity (2007)
pressure (db)
longitude (°E)

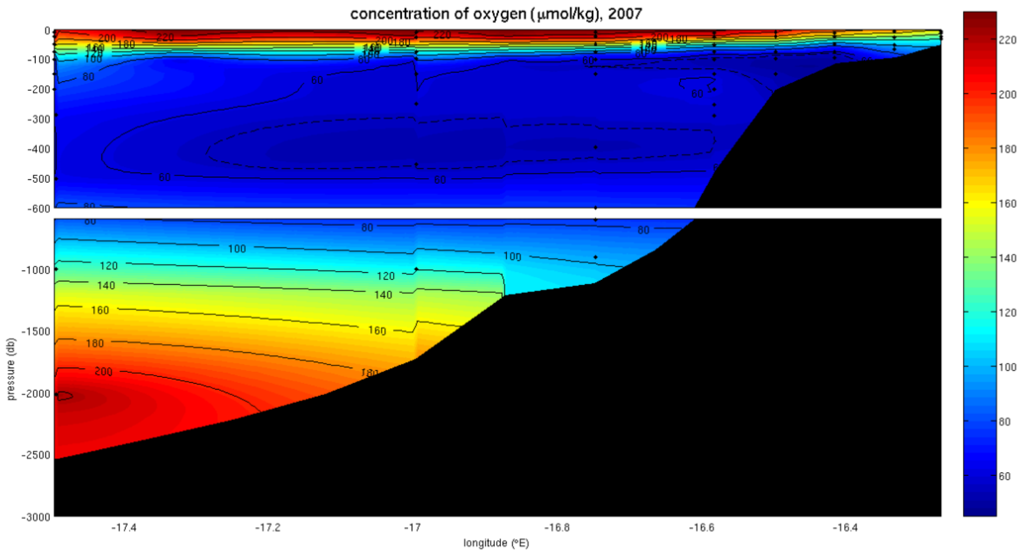
concentration of oxygen (μmol/kg), 2007
pressure (db)
longitude (°E)

Fig 3.1 Temperature, salinity and oxygen concentration for different years (2005, 2006, 2007) and different seasons (spring, summer, winter) are shown in this figure.

and SSS. Relative cooler and fresher water is transported from thermocline to the surface. As a result, the SST near the coast is lower than in the open ocean, and so is the SSS.
Between the depth of 150 and 600m, both temperature and salinity reduce smoothly to about 10 ℃ and 35.1, and the seasonal difference is not very large. North and South Atlantic Central Water contact here and mix with each other at this depth. No obvious zonal flow can be seen on the map.

2) Oxygen Distribution:
The surface oxygen concentration is high, especially in the open ocean. The NECC and NEUC transport water from south Atlantic and ventilate the eastern subtropical Atlantic.
Near the latitude of 18 °N the OMZ appears between 200 and 500 meter depth and near the coast (The dash lines shows the oxygen concentration lower than 60 µmol/kg.). This belongs to the North and South Atlantic Central Water.
In some coastal regions, the low concentration also appears between the depths of 100m and 200m (e.g. winter of 2007). This is because of the upwelling, which brings water from OMZ to the upper layer.

In the deeper layer:
1) Temperature and Salinity:
In the deeper layer, the lowest temperature is about 2 ℃ at the depth of 2000m. And the minimum of salinity is about 35 at the depth of about 1000m, in some stations, the values are even lower (as shown in the dashed lines). Low salinity can be an obvious sign to recognize AAIW. And NADW, which flows to the south, is relative warmer and has the higher salinity in the deep ocean.
2) Oxygen Distribution:
In the deeper layer, the oxygen concentration increases again because of the high solubility due to low temperature. The highest concentration in the deeper layer are found at the depth of about 2000m with a value of 200 µmol/kg.

3.2 Spatial and time difference in the upper layer

Since both upwelling and ventilation by NECC and NEUC happen in the upper layer, the upper 300m depth seems to be more interesting to us and the spatial and seasonal differences in the three years are shown in Fig 3.2. (Only data with CFC-12 and SF_6 are shown in the figures here, in order to keep synchronization with the mean age later.)
In summer (July and August, 2005), the stratification is clear. Besides the temperature (about 24 ℃ at surface), the salinity is also high (about 36.1) due to the strong solar

radiation and high evaporation. The concentration of oxygen in this season is relative low (about 200 μmol/kg at surface), because of the low solubility due to the high temperature, low ventilation and relative higher consumption of oxygen (will be discussed later in the AOU part). All the three parameters have relative strait contour lines and this shows that the convection is weak in this season and the impacts of NECC and NEUC cannot clearly be seen in the figure because of the lack of data (more details in the Discussion prat).

In spring (March and April, 2006), the seawater has the lowest salinity because the precipitation in this season is high. In the open ocean, the salinity at surface is about 36.0, and this value is even lower near the coast (between 35.6 and 35.8). The temperature is between summer and winter, 20 ℃ off-shore and 18 ℃ near coast at surface. The oxygen concentration is influenced by NECC and NEUC in the open ocean region, but weakly. They transport oxygen-rich water to the east until 17 °W, so the surface oxygen concentration in the west (west of 18 °W) is a litter higher but not very significant. Near the coast, the upwelling plays a more important role, water with lower oxygen concentration is brought up from the deep. The situation in spring is between winter and summer, and the upwelling in this season is high. (The upwelling near the coast cannot be seen very clear because of the lack of data.)

In winter (January, 2007), the temperature approaches its minimum. The SST in the off-shore region is about 20 ℃ and near the coast, it is even lower (about 17-18 ℃). The oxygen concentration is the highest (about 240 μmol/kg at surface in the open ocean, and about 200 μmol/kg near coast), because of the high solubility. The salinity is high in the off-shore region (about 36.1) but relative lower near the coast (about 35.8). The contour lines are the most tortuous, especially near the coast. These lines go up rapidly and show that, strong upwelling is induced there. NECC is relative stronger than spring at this time. Although there is no observational data west than 17.5 °W, we can still see that, the NECC transports surface water with high temperature, salinity and oxygen concentration to 16.5 °W. The upwelling near the coast is also clear. Water from about 100m depth is transported to the surface.

In general, the region, which longitude is west than 17 °W, has relative higher temperature, salinity and oxygen concentration. Surface water in this region is more influenced by currents (NECC and NEUC). The contour lines are relative strait and the stratification is also relative clear.

Near the coast, on the other hand, the contour lines are more curved than those in the open ocean. This shows that the vertical water exchange is more, upwelling is stronger and has a more important impact on the surface water. The seasonal difference is also larger.

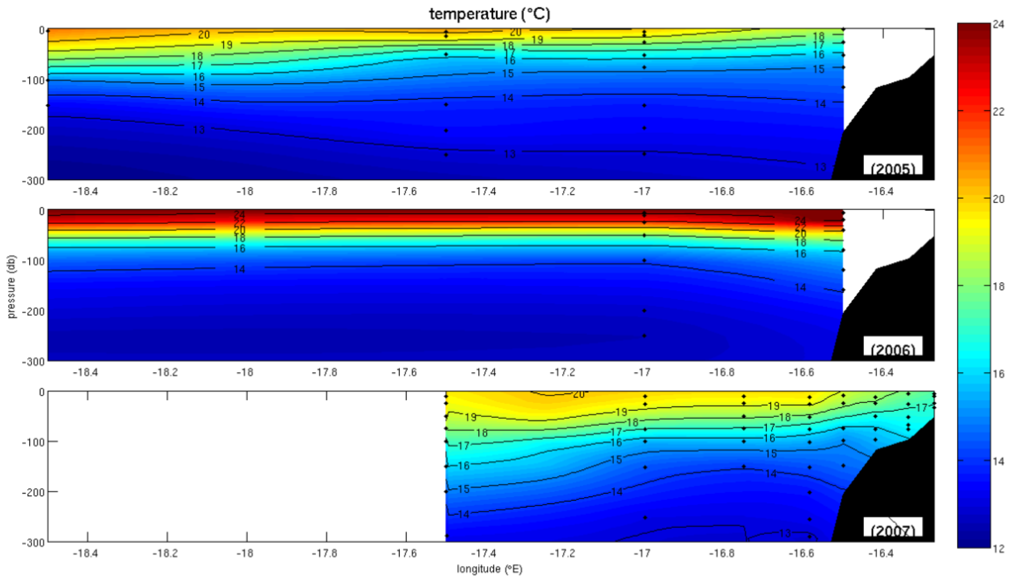
temperature (°C)
pressure (db)
longitude (°E)
(2005)
(2006)
(2007)

(a)

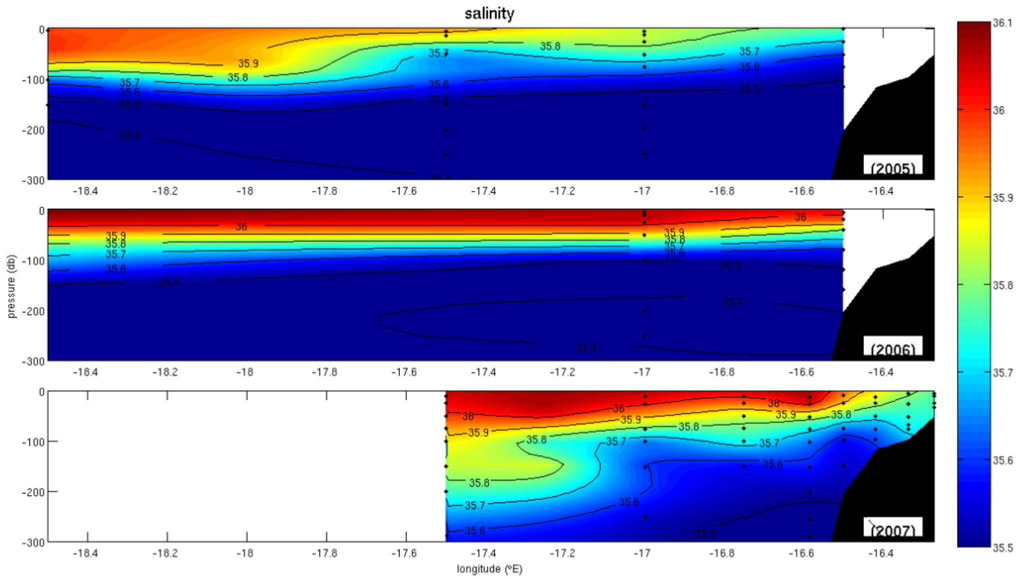
salinity
pressure (db)
longitude (°E)
(2005)
(2006)
(2007)

(b)

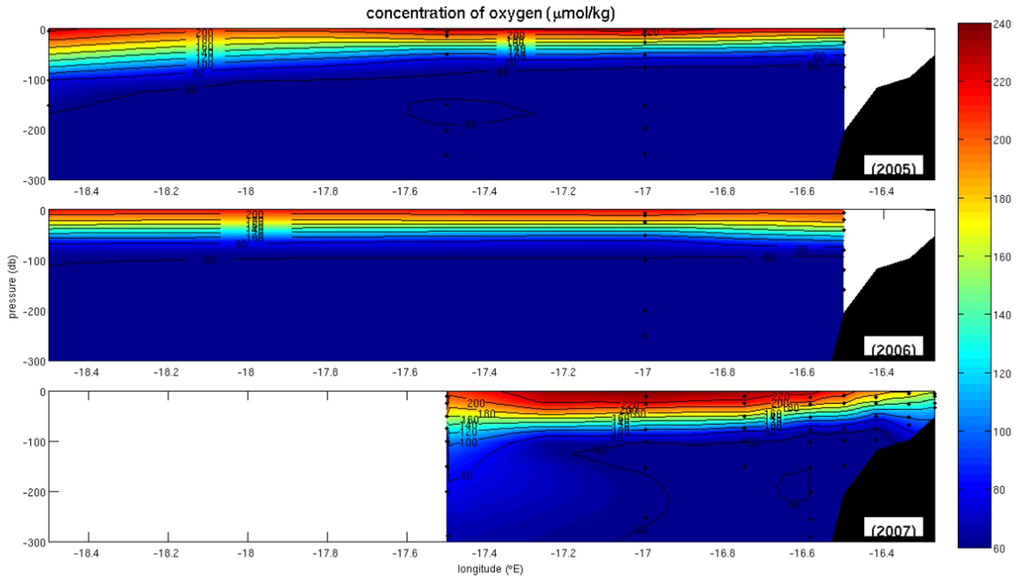

(c)

Fig 3.2 Spatial and seasonal differences in the upper 300m
Temperature (a), salinity (b) and oxygen concentration (c)
(Only data with CFC-12 and SF_6 are plotted)

3.3 Upwelling and ventilation based on tracer elements

The following measurements of upwelling and currents are based on conserved tracer elements (CFC-12 and SF_6). Before we look at the mean age of the water masses, some assumptions should be explained:
Firstly, we can show the measured concentration of each tracer element (CFC-12 and SF_6) as follows:

The concentrations of tracer gases (CFC-12 and SF_6) in seawater are similar with each other. The surface, which equilibriums to the present atmosphere, has the highest concentration. And the lowest concentration appears at the depth of about 2000m (see Fig 3.3).

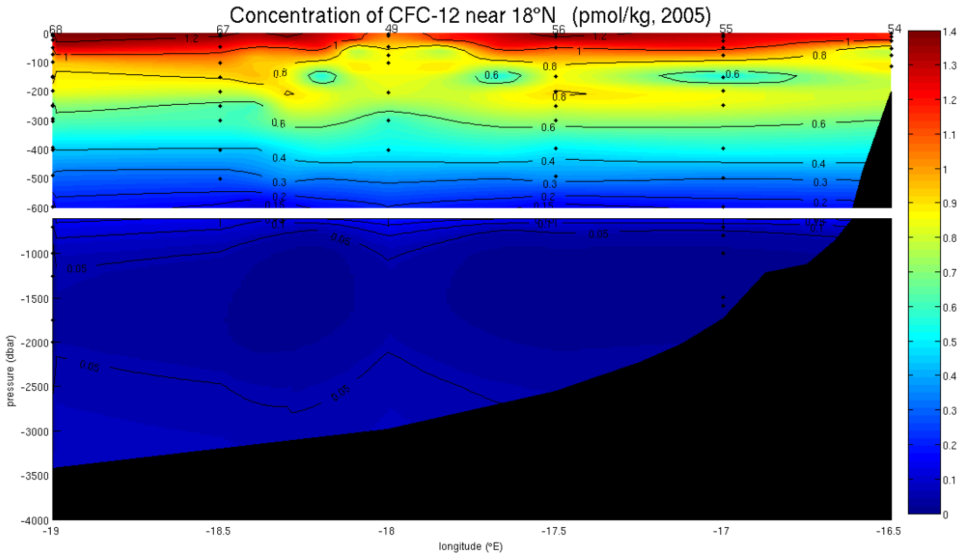
Concentration of CFC-12 near 18°N (pmol/kg, 2005)
pressure (dbar)
longitude (°E)

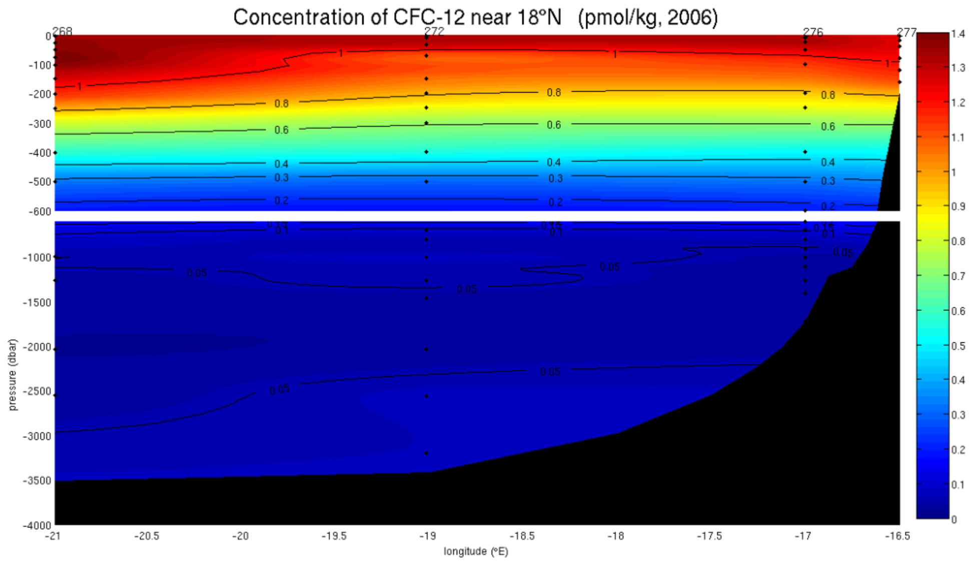
Concentration of CFC-12 near 18°N (pmol/kg, 2006)
pressure (dbar)
longitude (°E)

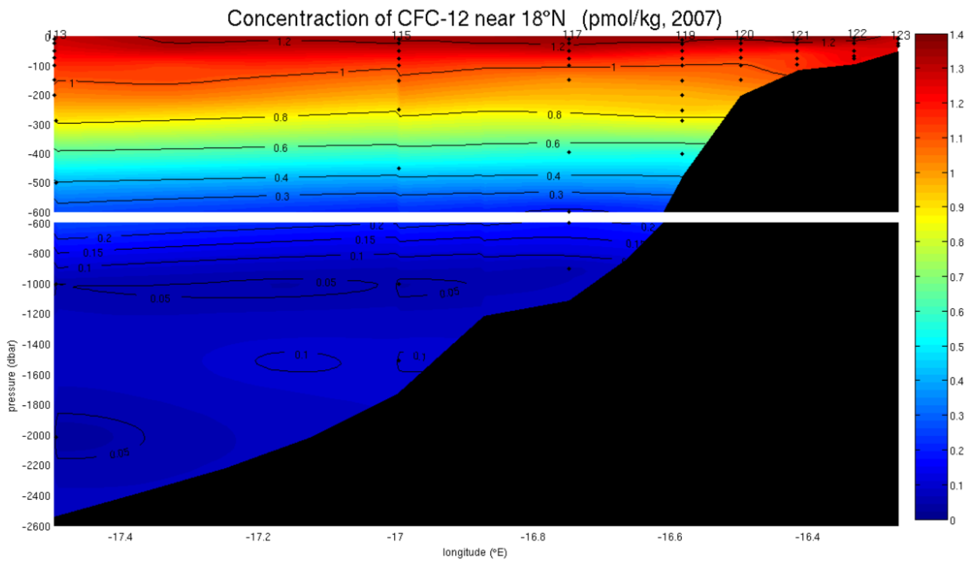
Concentraction of CFC-12 near 18°N (pmol/kg, 2007)
pressure (dbar)
longitude (°E)

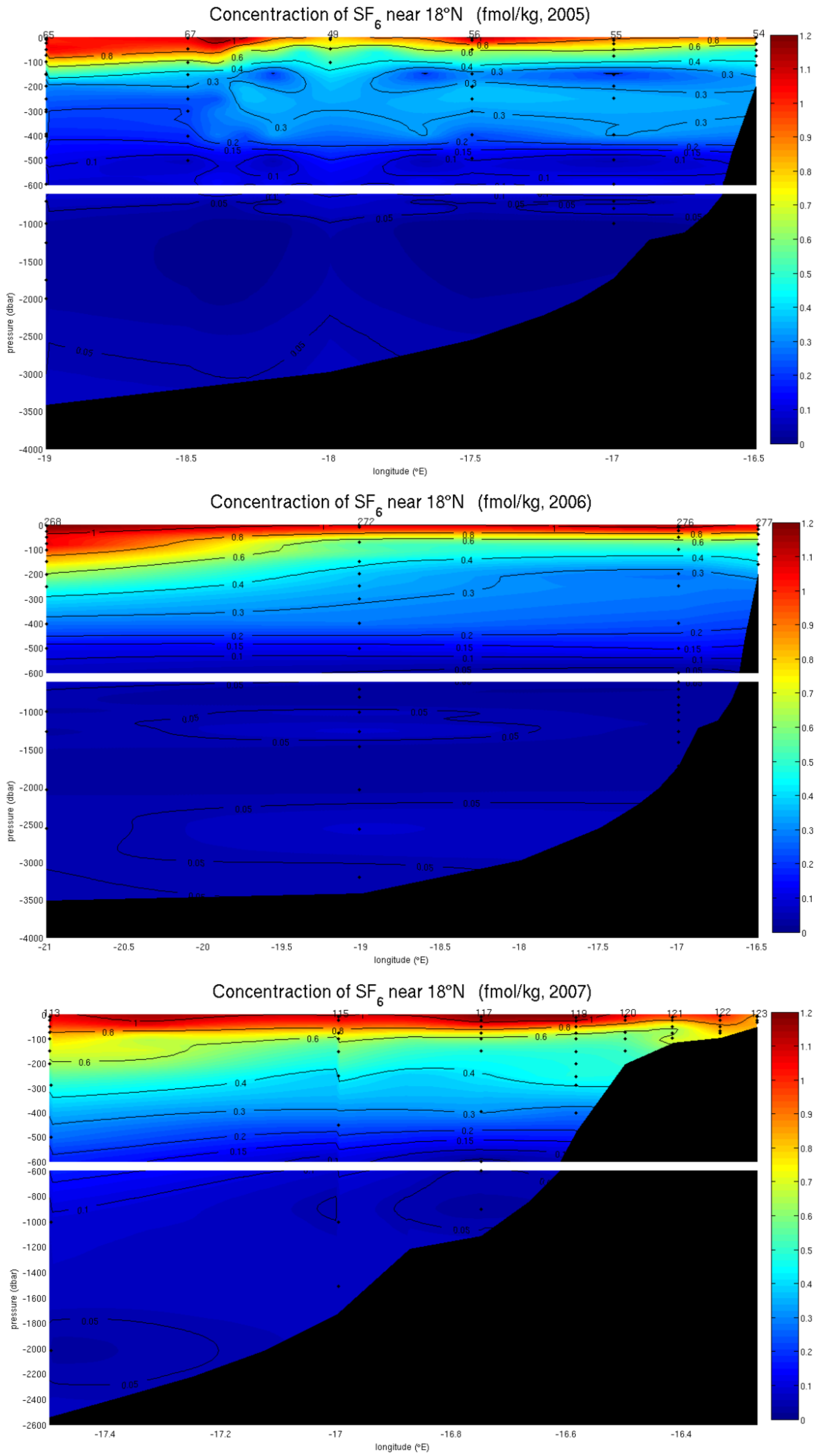

Fig 3.3 Concentration of CFC-12 (a) and SF_6 (b) of full depth

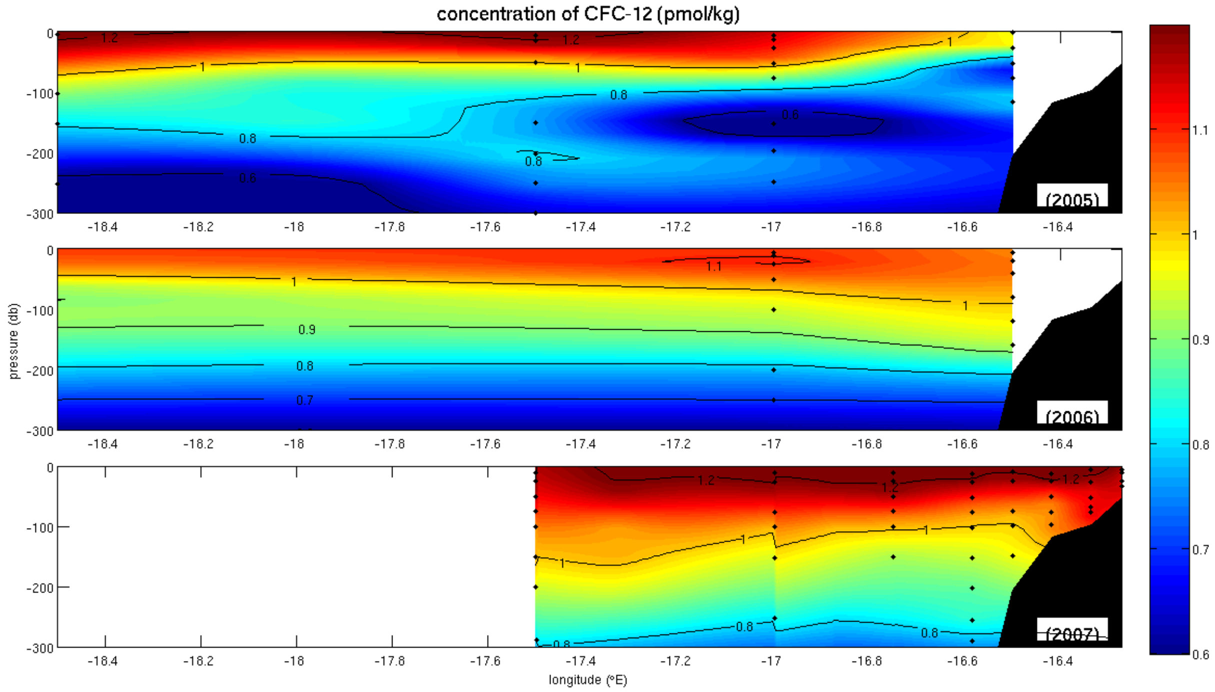

(a)

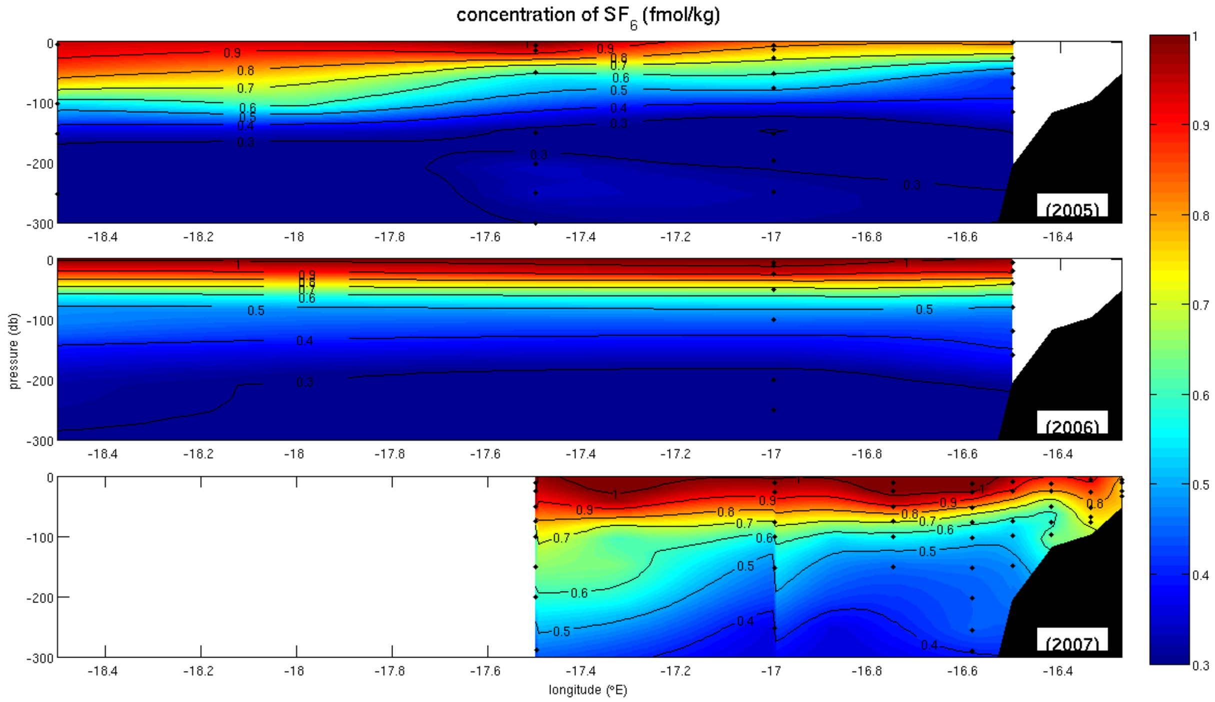

(b)

Fig 3.4 Concentration of CFC-12 (a) and SF_6 (b)

For CFC-12, the concentration is lowest in summer (about 1.1 pmol/kg) and highest in winter (about 1.2 pmol/kg), because the solubility decreases with temperature. For SF_6, the situation is a little different. The surface concentration of SF_6 in winter is also highest (higher than 1.1 fmol/kg), but the lowest concentration appears in spring instead of summer (about 0.9 fmol/kg). The reason could be the annual gradient of SF_6 during these three years.

The concentration we have now shows us the distribution of tracer gases in the seawater, but they are from different seasons (spring, summer and winter). So it is difficult to compare them with each other directly, since the potential temperature and salinity are different. As a result, the calculation of partial pressure is required.

Partial pressure of the dissolved gas in seawater means the partial pressure of this gas, which would be released into the atmosphere in equilibrium to the seawater, at this temperature. It is a function of potential temperature and salinity, so that the influence from S and T will be removed if we use partial pressure instead of concentration.
In spring and winter, the concentration is higher than summer but the partial pressure is lower. The solubility is low due to high temperature in summer, so that more gas can be released and equilibrium to the atmosphere although the concentration in seawater is low.

As shown in Fig (3.5), for CFC-12, the surface partial pressure is high in summer (higher than 500 ppt), and low in winter and spring (between 490 and 500 ppt). For SF_6, the distribution of surface partial pressure is similar: high in summer (about 6 ppt), low in spring (about 5 ppt), and surface partial pressure in winter is between them, about 5.5 ppt.

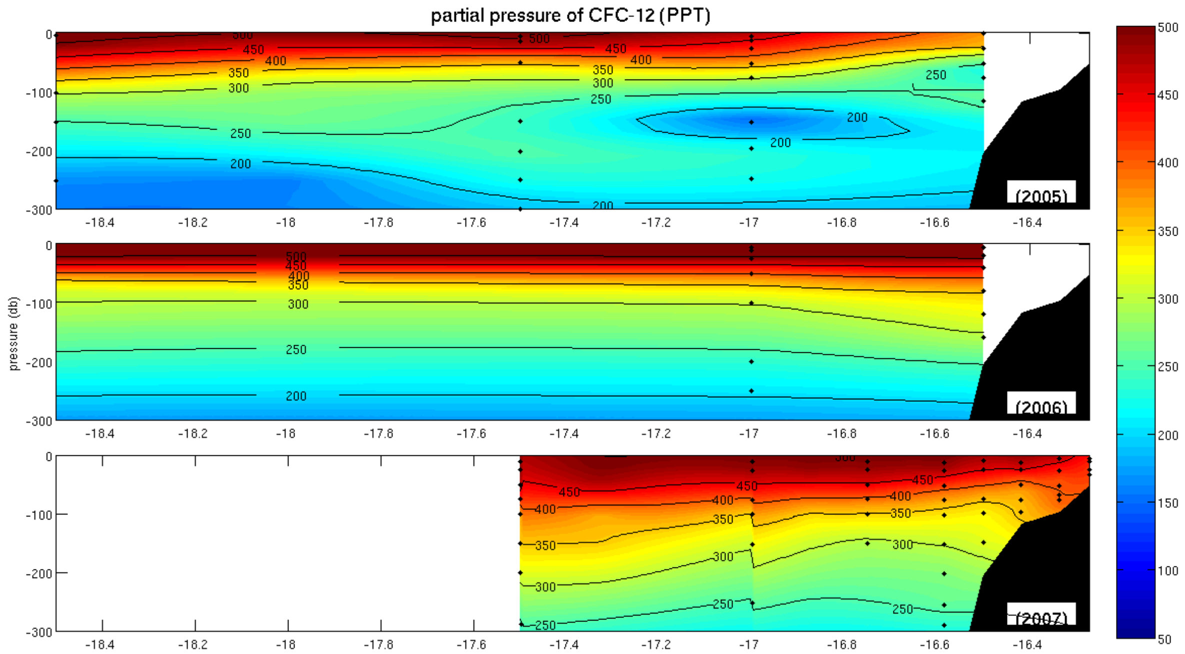

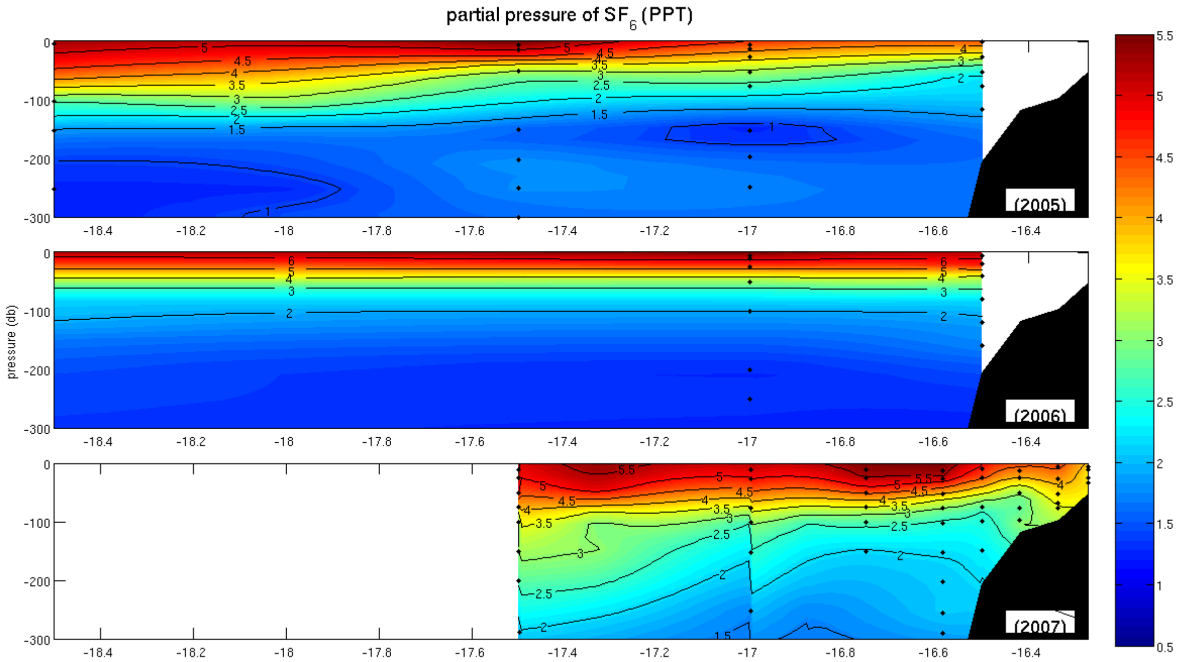

Fig 3.5 This figure shows us the partial pressure of CFC-12 (a) and SF_6 (b)
in seawater, which would be equilibrium to the atmosphere at the each temperature.

Now we have removed the impacts from temperature and salinity. But since the data we look at are in different years, partial pressure still has disadvantages to show the upwelling and currents, because the concentrations of these tracer elements in the atmospheric history are also different (mentioned in introduction part). Saturation is a result of partial pressure divided by the atmospheric concentration.

The increase of atmospheric concentration of CFC-12 slowed down since 1990s, and even decreases since middle 2000s, so the saturation in the year 2007 is higher than 2005 although the partial pressure is lower.

The atmospheric concentration of SF_6 increases monotonously, so the distribution of saturation is similar to partial pressure but a relative lower in the later years, compare with partial pressure, especially in 2007.

Fig 3.6 shows us the surface saturation at these stations, we can see values in coastal region (east of 17 °W) are relative lower than those in the open ocean area. This can be considered as a sign of the upwelling (More details will be discussed in the Discussion Section).

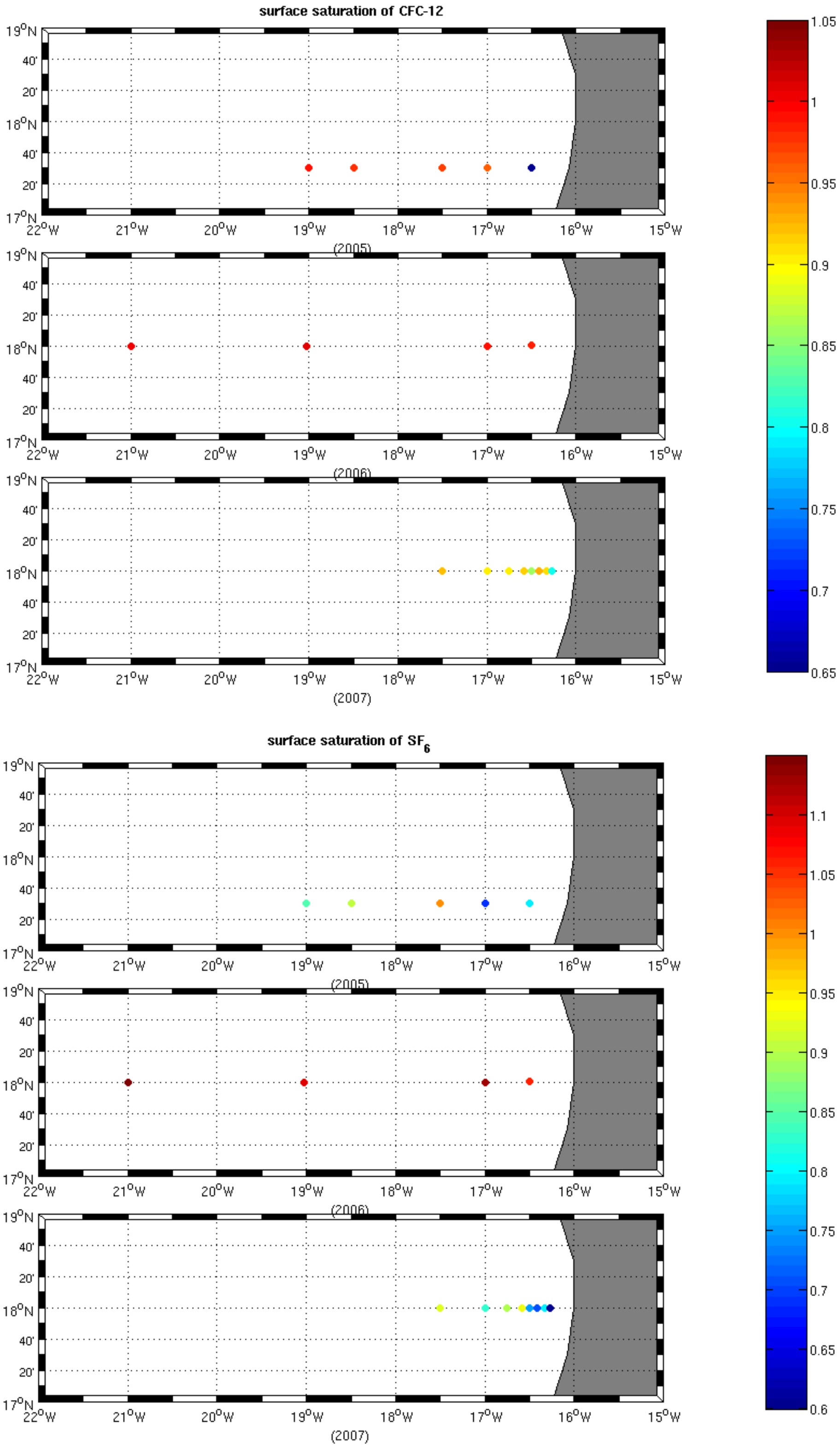

Fig 3.6 Surface saturation of CFC-12 (a) and SF_6 (b) measured in each station (2005 in spring, 2006 in summer, 2007 in winter)

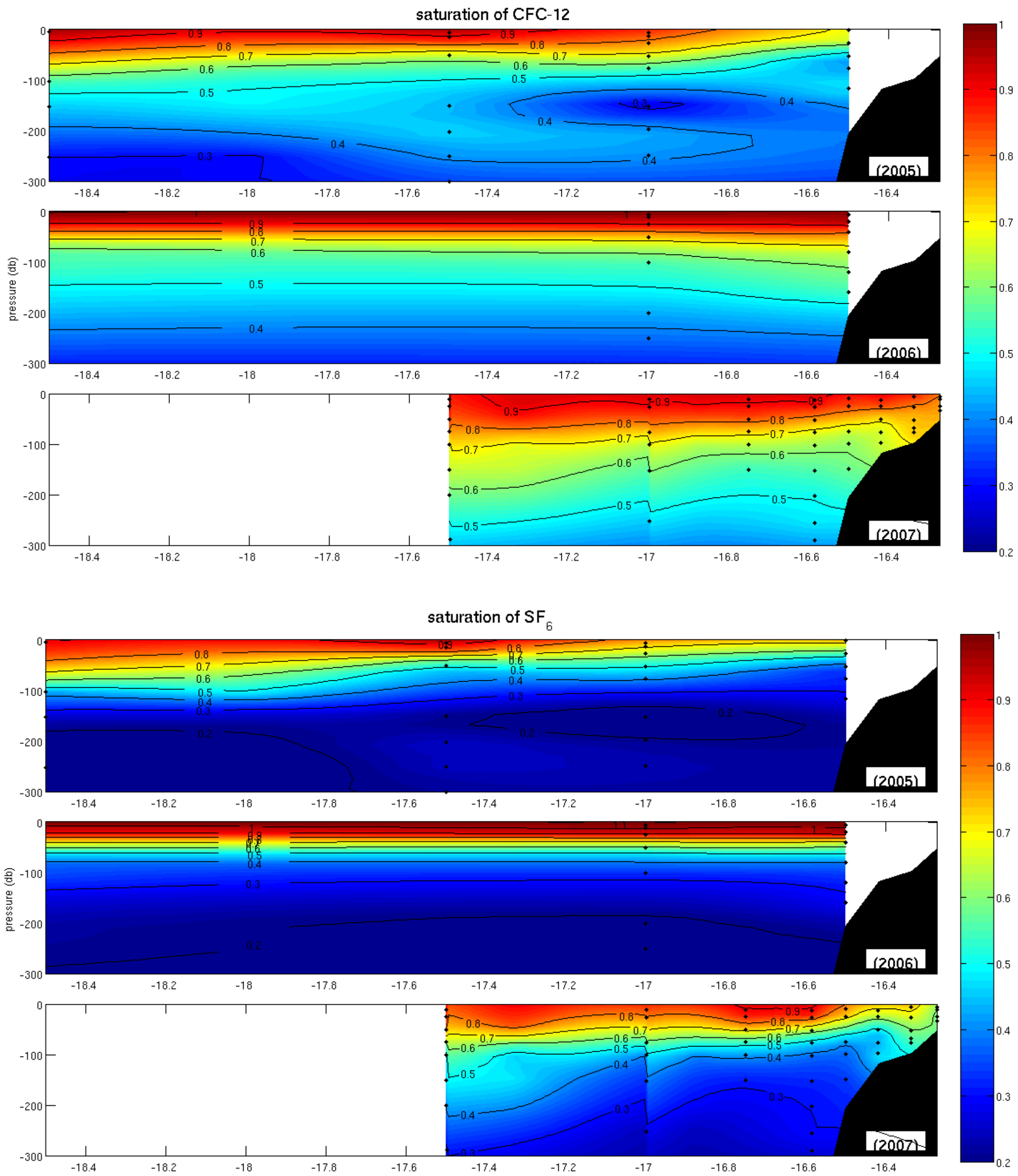

Fig 3.7 Saturation of CFC-12 (a) and SF_6 (b) in seawater are shown in this figure.

For both CFC-12 and SF_6, the saturation at surface is highest in summer (1.0 for CFC-12 and 1.1 for SF_6) due to the high temperature. The difference between spring and winter is not very large (about 0.9 for both tracer elements).

Finally, we get the mean age of the water masses as follows (Fig 3.8):
As mentioned in the introduction section, mean ages are based on CFC-12 in the old water masses and based on SF_6 in new formed water masses. Water mass with old mean age

(larger than 100 years) appears at the depth of 150m in spring of 2005. In summer of 2006, the stratification is clear. And near the coastal region (east of 17 °W), surface water is older (between 20 and 40 years) than the open ocean (between 0 and 20 years), especially in winter of 2007.

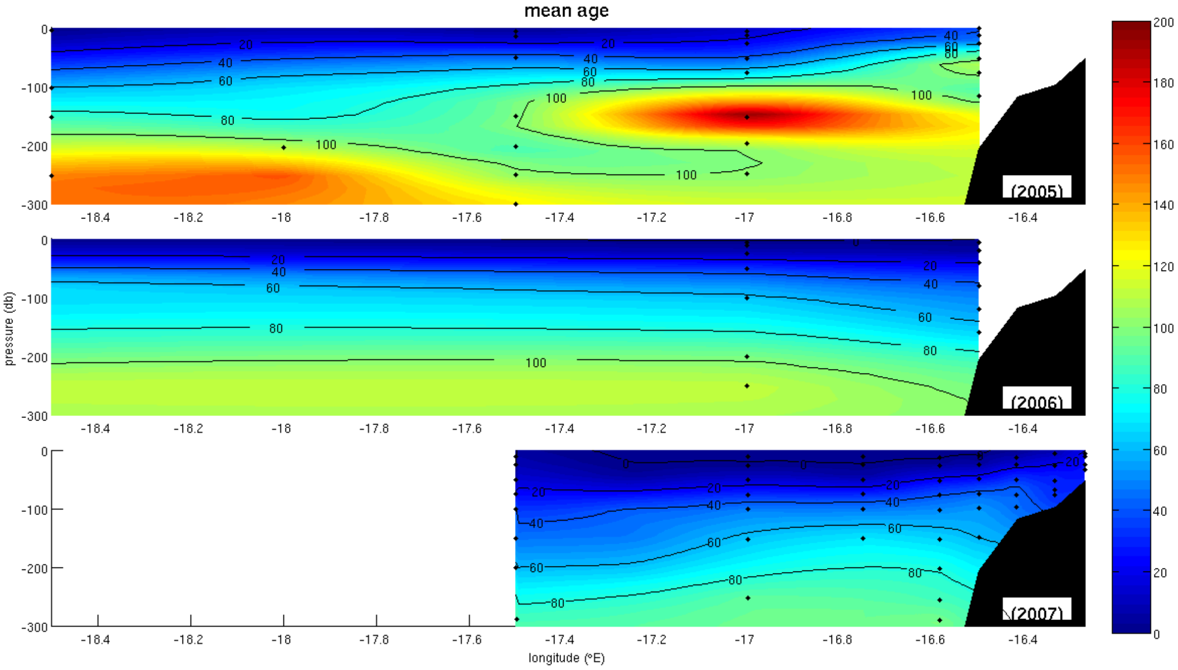

Fig 3.8 The mean ages of water masses in three years and seasons.
(Upper: spring of 2005, Middle: summer of 2006, Under: winter of 2007.)

The mean age increases with depth, and the maximum appears at the depth of about 2000m. The map can be divided into two parts. In the open ocean (west than 17 °W), upwelling has weak influence. Near the coast (east than 17 °W), the vertical water exchange due to upwelling is obvious:

In spring, water samples with old mean age (larger than 100 years) are found in the shallow layer (about 150m) near the coast (station 055, 17 °W). It shows that coastal upwelling is strong in this season.
At surface, the contour line of 20 years ends at the latitude of 16.9 °W. Around the depth of 50m, the water mass between 20 to 40 years go further, but do not reach the coast, either. It shows that the impacts from NECC and NEUC are in the open ocean (west than 17 °W) and they do not ventilate the coastal region.

In summer, the stratification is clear. No significant indications (such as old water) are found to show the upwelling near the coast.
The contour lines are also smooth in the open ocean. It shows that the NECC and NEUC are also very weak in summer and have small impact on the region.

In winter, stratification is relative clear in the open ocean, but near the coastal region, some relative older water samples with mean age of 20 to 40 years are found at surface. It shows that the upwelling in winter is also strong and happens most near the coast.
At surface, the contour lines spread tortuous. It shows that NECC is very strong at this time and more water are transported to the east. The NEUC, at the same time, flows eastwards at a larger mixed depth, round 100m.

Now we have estimated the oxygen transport in subtropical Atlantic. Another reason that influences the oxygen concentration is the consumption.

3.4 Apparent Oxygen Utilization (AOU) and Apparent Oxygen Utilization Rate (AOUR)

The AOU (apparent oxygen utilization) and AOUR (apparent oxygen utilization rate) shows the consumption of oxygen and the rate at which the oxygen is consumed in the ocean. Most of the consumption happens in the upper 500m depth. Within this depth, the oxygen is used in the process of decomposition of organic matters. And below 500m, most of the decompositions are complete, so the AOUR is very low below this depth and finally turn to be zero.
The relationship between the AOUR and the pressure follows the Martin curve (Karstensen et al., 2008):

$$\mathrm{AOUR} = c_1 + c_2 \cdot \exp(-\lambda \cdot z)$$

where c1, c2 and λ are constants, z is the pressure

In Mauritanian upwelling region, values of $c_1 = 0.06$, $c_2 = 4.7$ and $\lambda = 0.0035$ fit the AOUR distribution best (see Fig 3.9, red curve).

The seasonal difference can also be seen:
In spring of 2005 (black dots), the AOUR is lower than other two seasons (summer of 2006 in green and winter of 2007 in blue). In the deep ocean (under 500m), the AOUR is low (less than 1 $\mu mol \cdot kg^{-1} \cdot yr^{-1}$).

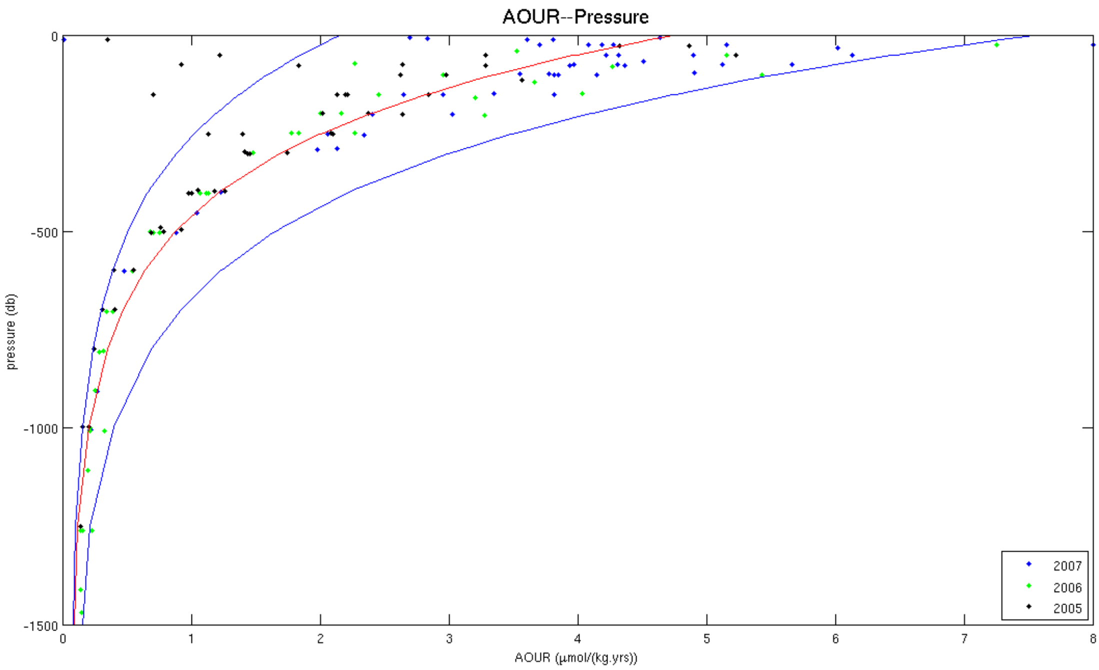

Fig 3.9 This figure shows us the relationship between AOUR and pressure in different seasons of three years. Black dots show the AOUR in spring of 2005, green dots show it in summer of 2006, and blue dots show it winter of 2007.

Table 3.1 Comparison between this thesis and result from Karstensen et al., 2008

		This Thesis	Karstensen et al., 2008
c1		0.06	-0.5
c2		4.7	12
λ		0.0035	0.0021
AOUR ($\mu mol \cdot kg^{-1} \cdot yr^{-1}$)	100m	3.37	9.23
	300m	1.70	5.89
	500m	0.88	3.70
	1000m	0.20	0.97
	1500m	0.085	0.014

4. Discussion

The environmental change, such as solar radiation and wind stress can lead to the variation of density of seawater, which is a function of temperature and salinity, and then influence the distribution and movement of water masses (e.g. upwelling and currents). Temperature, salinity and oxygen concentration can be directly measured. The movement of water masses can be inferred from TTD and the mean age of tracer gases.
In this section, seasonal variation of environment and their impacts will be discussed.

4.1 Impacts from solar radiation

The solar radiation has a direct impact on the temperature and salinity, especially at surface. There are two reasons, which influence the density of seawater, the temperature and the salinity. By warming up, the increase of temperature reduces the density. But during the evaporation, the density of surface water increases on the other hand.
In subtropical North Atlantic, the temperature has a more important impact than salinity on density of seawater at the surface. The seawater is heated and becomes lighter in the upper layer during the whole year, and the overturning circulation at surface in this region is polar-ward, but seasonal differences also exist:

In summer, the solar radiation is the highest. As a result, the surface water warms fast and the evaporation is also high. Since the temperature has a larger influence than salinity, the density of surface water is relative low and the stratification is clear. Less upwelling and vertical water exchange can be found in this season. Also, the high temperature due to the high radiation leads to a low solubility and high consumption, so the concentration of oxygen is low.

In winter, the solar radiation is weak, and the ocean loses heat to the atmosphere. The density at surface increases and induces the buoyancy loss. The stratification is weaker especially near the coast, where the temperature is lower than the open ocean. As a result, upwelling can easily be found in winter, especially near the coast. The oxygen concentration is high because of the high solubility and low AOUR.

In spring, the solar radiation and temperature is between summer and winter, so is the oxygen concentration. The AOUR is highest in spring because the high photosynthesis in this season. More oxygen is produced at surface (euphotic layer). But the solubility plays a more important role, so the oxygen concentration is still lower than winter.

In general, the seasonal variability of temperature and salinity is directly influenced by the solar radiation. Also, radiation can change the density of surface water and then influence the stratification and vertical water exchange. In the coastal region, the wind stress induced by difference capacity between continent and ocean has certain impact on the upwelling (This will be discussed later.). The oxygen concentration is also influenced by radiation. The solubility is a function of temperature. And the AOUR is a function of oxygen-consumption and photosynthesis, which is decided by solar radiation.

4.2 Impacts from wind stress

As mentioned before, upwelling near the coast is induced by wind stress. Besides the solar radiation, the physical processes, (including the currents and the ventilation processes, which are also induced by wind), can also decide the oxygen concentration in subtropical Atlantic.

So the importance of wind stress is clear in the following three aspects:

Impacts on upwelling:

Coastal upwelling is influenced by trade winds (Mittelstaedt, 1983). During the winter and early spring, the trade winds blows from northeast and the strength is high, cover the Mauritanian coast (see Fig 1.0 (c) left). The Ekman transport is induced by the wind and the surface water is transported westward, away from the coast. Coastal upwelling happens to drive deep water to the surface. In summer, the situation is different. Trade wind from northeast, cannot cover this region (see Fig 1.0 (c) right), and strength of the wind along the coast is low (see Fig 1.0 (b) right). So the Ekman transport is weak and upwelling can hardly be seen during summer.

Upwelling process can be inferred from the trace gases. Water with old mean age can be found in the shallow layer, especially near the coast, during winter and spring. But in summer the mean age of seawater increases with depth.

Impacts on currents:

Currents are also influenced by trade winds (Stramma et al., 2005). The NECC, which ventilates the eastern subtropical Atlantic basin, is induced by trade wind in this region. During the summer, the north boundary of ITCZ is in the north (Philander et al., 1995). The trade winds come from southeast, across the equator. According to the Sverdrup theory, they drive the surface water eastwards; the trade winds from northeast, at the same time, drive the surface water to the west. A divergence is formed in the east and the sea level is higher in the west. As a result, currents are induced from west to east in summer and reach their maximum in autumn. During the winter time, the north boundary of ITCZ is near the equator, so the trade winds from southeast cannot reach this region and the currents get weaker and finally disappear (Schott et al., 2004). This ventilation process is stronger in summer than in winter and it reduces the seasonal difference of oxygen concentration. However, low solubility due to high temperature plays here a more important role, so the oxygen concentration is still low in summer.

Ventilation process cannot also be clearly inferred from the tracer gases, because the horizontal water masses have similar mean age.

Impacts on precipitation and salinity:
The salinity in subtropical ocean is also influenced by trade wind. The surface water at subtropical is relative warmer and the evaporation is stronger. The clouds are As a result, the precipitation is lower in subtropical due to the trade winds and the salinity here is high. In zonal scale, the trade winds blow surface water to the west, and the precipitation there is stronger than the eastern area.

4.3 Comparison between the coastal region and the open ocean area

According to the analysis of mean age, this region can be divided into two parts, coastal region and open ocean area, by the longitude of 17 °W. The differences between coastal region and the open ocean area are as follows:

The first difference is the directions of water movement:
In the coastal region, the monsoon plays a more important role in the upper layer, while the trade wind influences the open ocean better. The monsoon transports the surface water away from the coast in winter and spring, so the upwelling happens in these seasons and the vertical water exchange is strong, especially in winter and early spring. The eastern subtropical Atlantic area is relative separated and less ventilated because the NEC and SEC do not go through this area and the currents (NECC and NEUC) which come from the west have less impact here than in the open ocean area. The upwelling and the vertical water exchange is the characteristics of the water motion in this area.
In the open ocean area, the wind stress cannot induce the upwelling because no Ekman divergence happens there. But the trade winds can induce the currents to the east. The horizontal water transport and currents plays the dominate role in the open ocean area, and the main direction of water movements in this area is horizontal.

The secondary difference between these two regions is the seasonal variability:
The coastal region has a larger seasonal variation in the upper layer, while the open ocean is more stable.
For example: The temperature in the coastal region has a variation of 7 ℃ (17 ℃ to 24 ℃), compared with 4 ℃ (20 ℃ to 24 ℃) in the open ocean area. This is due to different capacities between content and ocean. The land warms and cools faster respectively in summer and winter and the coastal region is influenced by land. The variation of salinity has the similar situation.

The third difference is the ventilation process:
The coastal region is located in the ‘‘shadow zone’’, where is less ventilated by the currents from the west and has the low oxygen concentration. The upwelling brings water from

OMZ to the surface so the oxygen becomes even lower.
In the open ocean area, the NECC and NEUC carry relative oxygen-rich water from the west. But compared with the NEC and SEC, the oxygen-concentration is still lower, because the strength of NECC and NEUC is weaker.
The eastern subtropical Atlantic is relative separated and less ventilated because the NEC and SEC do not go through this area, and NECC and NEUC come from the west. (More details about oxygen concentration will be discussed in the following paragraph.)

Saturation of tracer gases is also different between these two regions. Near the coastal region, the saturation, especially at surface (see Fig 3.6), is lower than the open ocean area in same season at the same latitude. Upwelling can be seen through the surface saturation to some extent. According to the relationship of saturation and mean age (Waugh et al., 2003), we can see that water with low saturation at surface has larger mean age. This means that deeper water is transported to the surface by the upwelling in the coastal region.

4.4 Distribution of oxygen

The Mauritanian upwelling region is in the eastern part of subtropical Atlantic and belongs to the Guinea Dome (shown in Fig 1.0), which is called ‘‘shadow zone’’ and has a low oxygen. So the oxygen situation near the Mauritania is similar as Guinea Dome, which is described by Karstensen et al., 2008. But differences also exist in the coastal region due to the upwelling, especially in winter and spring.

OMZ:
Result in this thesis is similar with the results from Karstensen et al., 2008. The deepest OMZ appears at the depth of about 500m, with a value of less than 60 µmol/kg. And the ventilation process is dominated by the NECC and NEUC. The differences also exist, especially in near the coastal region. Seawater from OMZ can also be found at the depth of 200m, because of the upwelling. And in the coastal region, the upwelling has a larger impact on the oxygen concentration rather than the currents.

AOUR:
The result of AOUR has also similarities with the result from Karstensen et al., 2008. The AOUR follows the Martin Curve and becomes nearly zero below 500 m depth.
The difference is that, the mean age is used in this thesis instead of tracer age. The AOUR in this thesis is lower except 1500m, since the mean age is used instead of tracer age. The advantage to use the mean age is that the tracer age underestimated the ‘‘true’’ age of the water mass (see Table 3.1). And the relationship between mean age and tracer age is shown in the introduction section (see Fig 1.3).

4.5 Uncertainties

1. Lack of data: During the year 2005 and 2006, there was no data east than 16.5 °W, so the coastal upwelling cannot be seen very clearly. Especially in the year 2006, data from only 4 stations includes the tracer gases and the distances between them are relative large. For example: Station 268, 272 and 276 (2006) across the longitude of 21 °W and 17 °W, without data of tracer gases between them. So upwelling between these stations cannot be measured based on tracer gases.

2. Analytical uncertainties: The concentration of tracer gases are very small, so the standard deviation is relative large.
   For example: During the cruise M68 (summer 2006), the error of CFC-12 could be 0.98 ppt, and the standard deviation is about 1.4%. For SF_6, the error is about 0.01 ppt, but the standard deviation could be as high as 5% since the partial pressure of SF6 is only 2-5 ppt in the upper 300m.

3. Regional difference: Most of the stations with tracer data are on the latitude of 18.5 °N in the year 2005, while in the year 2006 and 2007 the stations are along the latitude on 18 °N. The latitude of 18.5 °N is closer to the central of ‘‘shadow zone’’ in the south, so the oxygen concentration might be lower than the latitude on 18 °N under the same condition.

Reference

E. Barton. Eastern boundary of the North Atlantic: Northwest Africa and Iberia. In: Regional Studies and Syntheses 11, The Sea: The Global Coastal Ocean, A. Robinson und K. Brink, Hg., Wiley & Sons, New York, Pages 633–657, 1998.

B. Bourles, R. L. Molinari, E. Johns, W. D. Wilson, and K. D. Leaman. Upper layer currents in the western tropical North Atlantic (1989–1991). Journal of Geophysical Research, Vol. 104, No. C1, Page 1361-1375, 1999.

H. Bange et al, cruise report P320 unpublished, 8 pages., 2005.

P. Brandt, V. Hormann, A. Körtzinger, M. Visbeck, G. Krahmann, and L. Stramma. Changes in the Ventilation of the Oxygen Minimum Zone of the Tropical North Atlantic. Journal of Physical Oceanography, Vol. 40, Page 1784-1801, 2010.

H. Craig, and J.E. Lupton. Helium-3 and mantle volatiles in the ocean and the oceanic crust. Chapter 11 C. Emiliani (Ed.), The Sea, Vol. 7. The Oceanic Lithosphere, J. Wiley and Sons, Page 391–428, 1982.

L. Cao, K. Caldeira, and A. Jain. Effects of carbon dioxide and climate change on ocean acidification and carbonate mineral saturation. Geophysical Research Letters, Vol. 34, L05607, 2007.

M. Dengler, FS Poseidon cruise report P347, IFM-GEOMAR Report No. 16, 28 pages, IFM-GEOMAR, Kiel, 2008.

V. W. Ekman. On the influence of the earth's rotation on ocean currents. *Ark. Mat. Astron. Fys.*, Vol. 2 Page 1-53, 1905.

R. Fine. Observations of CFCs and SF_6 as Ocean Tracers. Marine Science, Vol. 3, Pages 173-195, 2011.

M. Gregg. Estimation and geography of diapycnal mixing in the stratified ocean. Physical

Processes in Lakes and Oceans, Vol. 54, Pages 305–338, 1998.

A. Ganachaud, and C. Wunsch. Improved estimates of global ocean circulation, heat transport and mixing from hydrographic data. Nature 408, Page 453-457, 2000.

P. Hughes and E. Barton. Stratification and water mass structure in upwelling area off northwest Africa in April/May 1969. Deep-Sea Research, Vol. 21, Issue 8, Pages 611–628, 1974.

I. Hamann, H. C. John and E. Mittelstaedt. Hydrography and its effect on fish larvae in the Mauritanian upwelling area. Deep-Sea Research Part a-Oceanographic Research

Papers, Vol. 28, Issue 6, Pages 561–575, 1981.

P. M. Holligan, R. D. Pingree and G. T. Mardell. Oceanic solitons, nutrient pulses and phytoplankton growth. Nature, Vol. 314, Issue 6009, Pages 348–350, 1985.

W. Hazeleger, P. Vries and Y. Friocourt. Sources of Equatorial Undercurrent in the Atlantic in a High Resolution Ocean Model. Journal of Physical Oceanography, Vol. 33, Issue 4, 2003.

A. Koschinsky, P. Brandt, and A. Körtzinger, Tropical Atlantic 2006: Meteor Cruise 68, April 26 August 7, Meteor-Berichte, 09-4, 188 pages, 2006.

T. Kuhlbrodt, A. Griesel, M. Montoya, A. Levermann, M. Hofmann, and S. Rahmstorf. On the driving processes of the Atlantic meridional overturning circulation. Reviews of Geophysics, Vol. 45, RG2001, 32 Pages, 2007.

J. Karstensen, L. Stramma and M. Visbeck. Oxygen minimum zones in the eastern tropical Atlantic and Pacific oceans. Progress in Oceanography, 77, 331-350, 2008.

A. Kock, J. Schafstall, M. Dengler, P. Brandt and H. Bange. Sea-to-air and diapycnal nitrous oxide fluxes in the eastern tropical North Atlantic. Biogeosciences Discussions, 8, 10299-10246, 2011.

R. Müller. Radioisotope dating with a cyclotron. Science, No. 4289, Vol. 196, 1977.

E. Mittelstaedt and I. Hamann. The coastal circulation off Mauritania. Deutsche Hydrographische Zeitschrift, Vol. 34, Issue 3, Pages 81–118, 1981.

E. Mittelstaedt. The upwelling Area off northwest Africa - a description of phenomena related to coastal upwelling. Progress in Oceanography, Vol. 12, Pages 307–331, 1983.

E. Mittelstaedt. The ocean boundary along the northwest African coast: Circulation and oceanographic properties at the sea surface. Progress in Oceanography, Vol. 26, Page 307-355, 1991.

C. Montégut, G. Madec, Albert, S. Fischer, A. Lazar, and D. Iudicone. Mixed layer depth over the global ocean: An examination of profile data and a profile-based climatology. Journal of Geophysical Research, Vol. 109, C12003, 20 Pages, 2004.

S. G. H. Philander, and J.-H. Yooh. Eastern Boundary Currents and Coastal Upwelling. Journal of Physical Oceanography. Vol, 12, Pages 862-878, 1982.

S. G. H. Philander, D. Gu, D. Halpern, G. Lambert, N.-C. Lau, T. Li, and R. Pacanowski. Why the ITCZ is mostly north of the equator. Journal of climate, Vol. 9, Page 2958-2972, 1995.

J. Price, R. Weller, R. Schudlich. Wind-Driven Ocean Currents and Ekman Transport. Science, New Series, Vol 238, No. 4833, 1534-1538, 1987.

A. Paulmier and D. Ruiz-Pino. Oxygen minimum zones (OMZs) in the modern ocean. Progress in Oceanography, Vol. 80, Pages 113-128, 2009.

A. Rees, I. Brown, D. Clark and R. Torres. The Lagrangian progression of nitrous oxide within filaments formed in the Mauritanian upwelling. Geophysical Research Letters, Vol. 38, 2011.

G. Siedler, N. Zangenberg,R. Onken, and A. Morlière. Seasonal Changes in the Tropical Atlantic Circulation: Observation and Simulation of the Guinea Dome. Journal of

Geophysical Research, C1,97 Pages 703-715, 1992.

L. Stramma and F. Schott. The mean flow field of the tropical Atlantic Ocean. Deep-Sea Research II, 46, 279-303, 1999.

L. Stramma, S. Hüttl and J. Schafstall. Water masses and currents in the upper tropical northeast Atlantic off northwest Africa. Journal of Geophysical Research, Vol. 110, 2005.

L. Stramma, G. Johnson, J. Sprintall and V. Mohrholz. Expanding Oxygen Minimum Zone in the Tropical Oceans. Science, Vol. 320, No. 5876, Page 655-658, 2008.

F. A. Schott, J. P. McCreary Jr., and G. C. Johnson. Shallow overturning circulations of the tropical-subtropical oceans. Geophysical Monograph Series, Vol. 147, Page 261-304, 2004.

J. Schafstall, M. Dengler, P. Brandt and H. Bange. Tidal-induced mixing and diapycnal nutrient fluxes in the Mauritanian upwelling region. Journal of Geophysical Research, Vol. 115, 2010.

R. Thomson, and I. Fine. Estimating mixed layer depth from oceanic profile data. Journal of Atmospheric and Oceanic Technology, Vol. 20, Issue 2, 2003.

T. Tanhua, D. Waugh and D. Wallance. Use of SF_6 to estimate anthropogenic CO_2 in the upper ocean. Journal of Geophysical Research, Vol. 113, 2008.

D. Waugh, T. Hall and T. Haine. Relationships among tracer ages. Journal of Geophysical Research, Vol. 108, 2003.

K. Yoshid. The coastal undercurrent— A role of longshore scales in coastal upwelling dynamics. Progress in Oceanography. Vol 9, Issue 2, Pages 83–131,1980.

C. Zindler, I. Peeken, C. Marandino and H. Bange. Environmental control on the variability of DMS and DMSP in the Mauritanian upwelling region. Biogeosciences, 9, 1042-1051, 2012.

Acknowledgement

First of all, I must thank my advisers Prof. Dr. Martin Visbeck and Dr. Toste Tanhua for the chance to study and write this thesis in GEOMAR. In particular, I must thank Dr. Toste Tanhua for always taking interest in my thesis and ensuring its continued progress, for his guidance and his enthusiasm. With their help, it is possible for me to finish my thesis.

I would like to thank Dr. Hermann Bange for his support and information of the cruise report, taking the samples during the 2005 and 2006 cruise. Thanks to Anke Schneider for measuring the samples.

I must also thank Prof. Dr. Noel Keelnyside, Prof. Dr. Richard Greatbatch and other Tutors for their teachings during my study in these two years as a Master student in GEOMAR.

I would also like to thank our department secretary Cordula Zenk for her help during my staying here. Especially, she gave me so great help in dealing with all of the procedures when I came here initially. And thank everybody in our department for their help and their encouragement to me to study as a foreign student in Germany.